Catal Surv Asia (2008) 12:38–55
DOI 10.1007/s10563-007-9038-9

Review of Ag/Al_2O_3-Reductant System in the Selective Catalytic Reduction of NO_x

Hong He · Xiuli Zhang · Qiang Wu · Changbin Zhang · Yunbo Yu

Received: 6 August 2007 / Accepted: 7 December 2007 / Published online: 3 January 2008

Abstract Ag/Al_2O_3 is a promising catalyst for the selective catalytic reduction (SCR) by hydrocarbons (HC) of NO_x in both laboratory and diesel engine bench tests. New developments of the HC-SCR of NO_x over a Ag/Al_2O_3 catalyst are reviewed, including the efficiencies and sulfur tolerances of different Ag/Al_2O_3-reductant systems for the SCR of NO_x; the low-temperature activity improvement of H_2-assisted HC-SCR of NO_x over Ag/Al_2O_3; and the application of a Ag/Al_2O_3-ethanol SCR system with a heavy-duty diesel engine. The discussions are focused on the reaction mechanisms of different Ag/Al_2O_3-reductant systems and H_2-assisted HC-SCR of NO_x over Ag/Al_2O_3. A SO_2-resistant surface structure in situ synthesized on Ag/Al_2O_3 by using ethanol as a reductant is proposed based on the study of the sulfate formation. These results provide new insight into the design of a high-efficiency NO_x reduction system. The diesel engine bench test results showed that a Ag/Al_2O_3-ethanol system is promising for catalytic cleaning of NO_x in diesel exhaust.

Keywords Ag/Al_2O_3 · Hydrocarbon · HC-SCR · NO · SO_2 · Hydrogen · Mechanism · Diesel engine

1 Introduction

Air pollution by nitrogen oxides (NO_x) emitted from both mobile and stationary sources has become a serious environmental problem because of the formation of acid rain and photochemical smog [1]. The three-way catalysts have been applied successfully to eliminate the NO_x from the gasoline engines. Although the improvement of fuel economy and lower emissions of CO_2 can be obtained by using diesel and lean-burn gasoline engines, the oxygen rich exhausts make the conventional three-way catalysts unsuitable for the reduction of NO_x emissions. As a highly promising technology, selective catalytic reduction (SCR) of NO_x with various reductants has been extensively studied. Since unburned HC and CO in exhausts of diesel and lean-burn gasoline engines are not enough to reduce NO_x, the additional reductant is needed. Besides the SCR of NO_x by NH_3 or urea as a reductant, the SCR of NO_x by hydrocarbon (HC) as a reductant can be a possible method to the removal of NO_x from diesel and lean-burn gasoline engines. In recent studies, relatively durable and inexpensive alumina-supported silver catalysts (Ag/Al_2O_3) have been considered to be a promising candidate for practical usage in the HC-SCR of NO_x [2–8]. In our research into the HC-SCR of NO_x over Ag/Al_2O_3, we found a novel enolic surface species on Ag/Al_2O_3 [9] and proposed a new mechanism to explain the high-level efficiency of the SCR of NO_x by ethanol over Ag/Al_2O_3 [7, 9, 10], as shown in Scheme 1. The reaction starts with the formation of nitrates adsorbed on Al_2O_3 via NO oxidation by O_2, and enolic species and acetate adsorbed on Ag and Al_2O_3 via the partial oxidation of C_2H_5OH on Ag/Al_2O_3 [7]. Subsequently, the enolic species can react with nitrates or $NO + O_2$ to form surface –NCO species adsorbed on Ag site (Ag–NCO) and Al site (Al–NCO) as a key intermediate directly, or via organo-nitrogen compounds (such as R-ONO and $R-NO_2$) [11]. Finally, Ag–NCO and Al–NCO species react with $NO + O_2$ and nitrates to yield N_2. It should be pointed

H. He (✉) · X. Zhang · Q. Wu · C. Zhang · Y. Yu
State Key Laboratory of Environmental Chemistry and Ecotoxicology, Research Center for Eco-Environmental Sciences, Chinese Academy of Sciences, P.O. Box 2871, 18 Shuangqing Road, Beijing 100085, P.R. China
e-mail: honghe@rcees.ac.cn

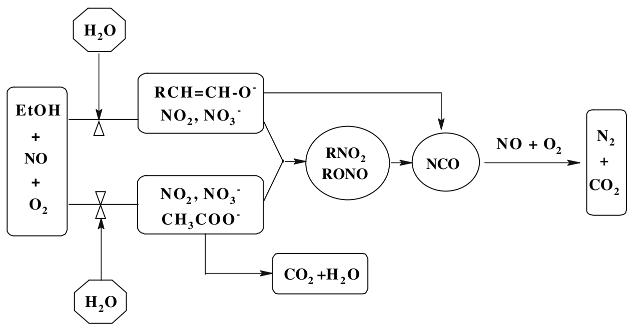

Scheme 1 The mechanism of the SCR of NO_x by C_2H_5OH over Ag/Al_2O_3

out that the enolic species, the main surface species during the partial oxidation of C_2H_5OH, has a higher reactivity with $NO + O_2$ to form surface –NCO species than acetate, which results in the high-level efficiency of NO_x reduction over Ag/Al_2O_3 by C_2H_5OH. Also, the role of the active phase Ag is to accelerate the formation of these above intermediates, and then these intermediates are finally transferred onto the support Al_2O_3. On the basis of these results, we concluded that C_{2+} oxygenated hydrocarbons are more efficient than hydrocarbons as reductants for the SCR of NO_x.

From a practical point of view, a catalyst used for the SCR of NO_x should be resistant to both SO_2 and H_2O in real exhaust gases; and the type of reductant is an important factor for the SO_2 and H_2O tolerances of Ag/Al_2O_3 during the SCR of NO_x. Previous studies have shown that Ag/Al_2O_3 was usually deactivated in the presence of SO_2 and H_2O during the HC-SCR of NO_x [12–16]. However, ethanol was extremely effective for the SCR of NO_x over Ag/Al_2O_3 even in the presence of H_2O and SO_2, which was confirmed by diesel engine bench tests [7, 17–19]. To achieve the practical use, a SCR catalyst should also have a high level of activity for NO_x reduction at lower temperature, considering the typical temperatures of diesel exhausts and cold-start driving cycle. Modification of the reaction atmosphere by adding H_2 to an HC-SCR system could be useful because of the surprising promotional effect on the SCR of NO_x over Ag/Al_2O_3 catalyst [20–22].

In this review, we summarize our recent studies of: (1) the mechanistic difference of the SCR of NO_x over Ag/Al_2O_3 using different reductants; (2) the SO_2 tolerance of a Ag/Al_2O_3-reductant system; (3) the promotional effect and mechanism of H_2-assisted HC-SCR of NO_x over Ag/Al_2O_3; (4) application of a Ag/Al_2O_3–C_2H_5OH–SCR system with a heavy-duty diesel engine. These results provide new insight into the design of the high-efficiency NO_x reduction system for practical use.

2 SCR of NO_x with Various Oxygenated Hydrocarbon Reductants Over Ag/Al_2O_3

2.1 Reaction Activity of Various Oxygenated Hydrocarbon Reductants for the SCR of NO_x Over a Ag/Al_2O_3 Catalyst

The efficiencies of different Ag/Al_2O_3-reductant systems for the SCR of NO_x were examined [23]. In the previous paper [7], the preparation of Ag/Al_2O_3 was described in detail, and an optimum loading of Ag on Al_2O_3 (around 4 wt.%) was confirmed. Therefore, the 4 wt.% Ag/Al_2O_3 catalyst was adopted in this review. The reductants used here were classified as: C1 (CH_3OH, dimethyl ether (DME)), C2 (C_2H_5OH, CH_3CHO), C3 (C_3H_6, isopropyl alcohol (IPA), 1-propanol and acetone) and C4 (1-butanol). Figure 1 shows the NO_x conversions with various reductants over Ag/Al_2O_3. High-level conversions of NO_x were achieved in the temperature range of 473–773 K when using C2, C3 and C4 reductants. In the case of C1 reductants, it is worth noting that the level of NO_x conversion was much lower than those of using C2, C3 and C4 as reductants under the same conditions. The results indicate that conversion of NO_x over Ag/Al_2O_3 is influenced strongly by the reductants, and the efficiency order of the reductants for the SCR of NO_x over Ag/Al_2O_3 is proposed as follows: C4 $\approx$ C2 > C3 >> C1.

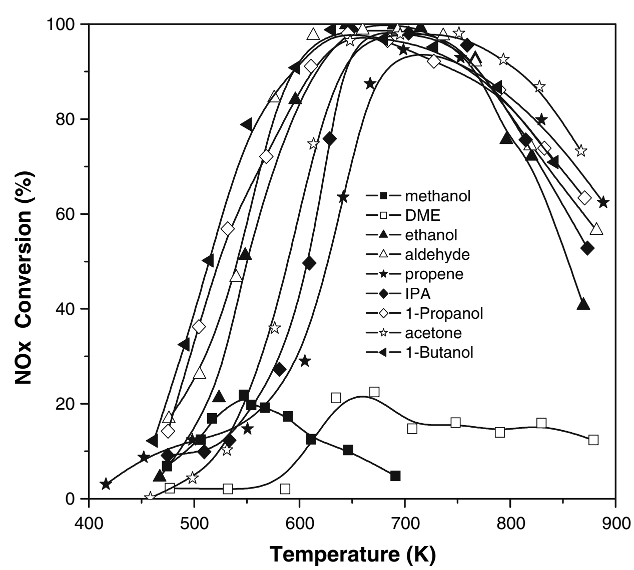

Fig. 1 Activities of 4 wt.% Ag/Al_2O_3 for the SCR of NO_x with various reductants. Conditions: NO, 800 ppm; O_2, 10%; H_2O, 10%; reductants (methanol 3,030 ppm or DME 3,030 ppm or ethanol 1,565 ppm or acetaldehyde 1,565 ppm or propene 1,714 ppm or IPA 1,043 ppm or 1-propanol 1,043 ppm or acetone 1,043 ppm or 1-butanol 783 ppm) in N_2 balance at a total flow rate of 2,000 cm^3/min, GHSV = 50,000 h^{-1}

2.2 Reaction Mechanism of the SCR of NO_x by Various Reductants Over Ag/Al_2O_3

It is well known that the reaction mechanism of the SCR of NO_x depends mainly on the type of catalyst, the identity of reagents, the type of reductant, and the reaction conditions [24–27]. So far, researchers have agreed that the –NCO species acts as the key intermediate during the SCR of NO_x, and its high reactivity with NO + O_2 results in a highly efficient reduction of NO_x [7, 9–11, 15, 16, 21, 28–31]. We recently proposed a novel mechanism for the SCR of NO_x by C_2H_5OH, as shown in Scheme 1, where the surface enolic species is related to the high surface concentration of –NCO and the high efficiency of NO_x reduction by C_2H_5OH [7, 9, 10]. In order to clarify the high activity of enolic species towards NO + O_2 to form –NCO, the dynamic changes of the surface intermediates on Ag/Al_2O_3 as a function of time have been investigated by using in situ DRIFTS measurement [10]. Figure 2 shows time dependence of the integrated area of the bands for different species in the DRIFTS spectra. A sharp decrease in the band due to enolic species was observed in a flow of NO + O_2 on Ag/Al_2O_3 after exposed to C_2H_5OH + O_2. The band assignable to enolic species sharply disappeared after 5 min with simultaneous formation of an –NCO band. Then band assignable to acetate slowly decrease after 5 min, showing the lower reactivity of acetate than enolic species. From the dynamic changes of these bands in a flow of NO + O_2, we conclude that enolic species on Ag/Al_2O_3 are highly active towards NO + O_2, resulting in the formation of the –NCO species which is the key reaction intermediate in the SCR of NO_x. This mechanism has already explained rationally the difference in the SCR of

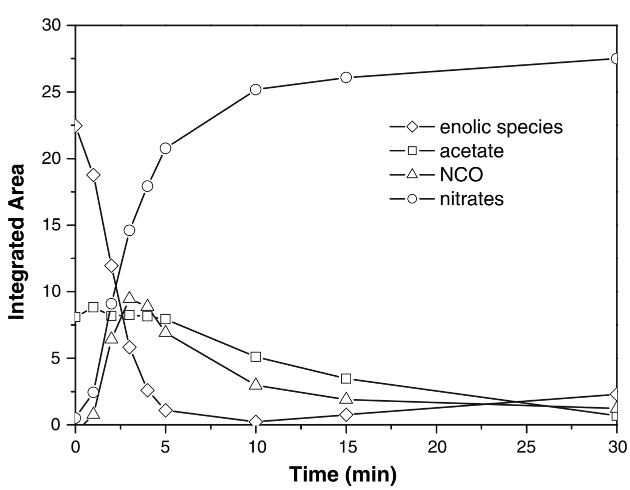

Fig. 2 Time dependence of the integrated area of the bands in a flow of NO + O_2 at 673 K. Before the measurement, the catalyst was pre-exposed to a flow of C_2H_5OH + O_2 for 60 min at 673 K. Conditions: NO, 800 ppm; C_2H_5OH, 1,565 ppm; O_2, 10%

NO_x when using C_2H_5OH and C_3H_6 as reductants [10]. To obtain further theoretical information about the highly efficient catalyst–reductant system, it is very important to investigate the different reaction mechanisms of the SCR of NO_x with different reductants over Ag/Al_2O_3.

The difference between the above reductants for the SCR of NO_x over Ag/Al_2O_3 was investigated by the in situ DRIFTS method. As shown in Fig. 3a–e, the very strong peak at around 2,229–2,233 cm^{-1} is associated with the –NCO species adsorbed on Ag site of Ag/Al_2O_3 catalyst, as observed in other NO_x/O_2/hydrocarbon reactions [7, 9–11, 15, 16, 21, 28–31]. The peaks around 1,633–1,639 cm^{-1}, 1,412–1,416 cm^{-1} and 1,336–1,338 cm^{-1} are assigned to the surface enolic species derived from the partial oxidation of C2–C4 reductants over Ag/Al_2O_3 [7, 9, 10, 23, 32]. The enolic species has a crucial role in the –NCO formation during the SCR of NO_x [7, 9, 10, 23]. In addition, the strong peaks around 1,572–1,579 cm^{-1} and 1,464–1,468 cm^{-1} are assigned to the acetate species, and the peaks around 1,585–1,589 cm^{-1} and 1,300–1,304 cm^{-1} are due to the nitrates adsorbed on Ag/Al_2O_3 [7, 9, 10, 29–31]. The peaks around 1,591–1,595 cm^{-1}, 1,379 cm^{-1} and 1,390–1,392 cm^{-1} are assigned to the surface formate species formed from the partial oxidation of C1 reductants over Ag/Al_2O_3 (Fig. 3f and g) [23]. Based on the above results, we conclude that the formate species is main species in the partial oxidation of C1, while the enolic species is main species in the partial oxidation of C2–C4 reductants on the Ag/Al_2O_3 surface. The assignments of the main IR bands are summarized in Table 1.

As can be seen in Fig. 3f and g, the formation of –NCO species in the NO_x/O_2/C1 reductant reactions is different from those of the NO_x/O_2/C2–C4 reductant reactions. Taking the relationship between the concentration of –NCO and efficiency of NO_x reduction, for C2–C4 reductants, the high concentration of –NCO species should account for the corresponding highly efficient NO_x reduction. In addition, we cannot observe an obvious difference among those figures (Fig. 3a–e), indicating that C2, C3 and C4 reductants are likely to follow a similar reaction mechanism during the SCR of NO_x. As for C1 reductants, a very weak band of –NCO species was observed under the same experimental conditions, which can well explain the relatively low efficiency of the SCR of NO_x (Fig. 3f and g).

We have proposed the mechanism of the SCR of NO_x with C_2H_5OH and IPA over Ag/Al_2O_3, where the surface enolic species was found to be related to the high surface concentration of –NCO and the high efficiency of NO_x reduction [23]. Comparative studies showed that the partial oxidation of C1 reductants is different from that of C2–C4 reductants. It was found that formate was the main surface species during the partial oxidation of C1 reductants on Ag/Al_2O_3, and it had a low level of reactivity with nitrate

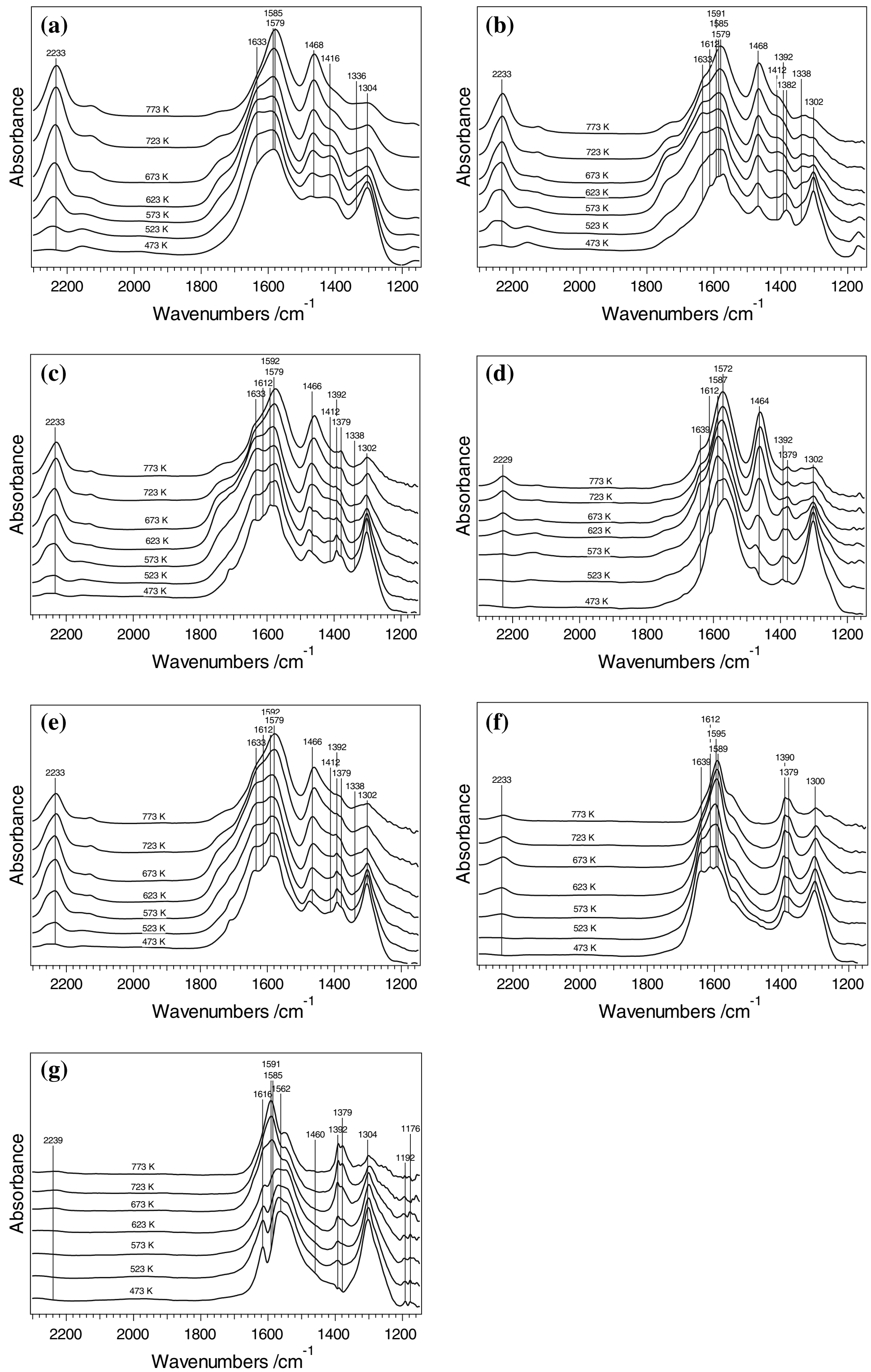

Fig. 3 (**a**) In situ DRIFTS spectra of adsorbed species in the steady state on 4 wt.% Ag/Al_2O_3 in a flow of $C_2H_5OH + NO + O_2$ at various temperatures. Conditions: NO, 800 ppm; C_2H_5OH, 1,565 ppm; O_2, 10%. (**b**) In situ DRIFTS spectra of adsorbed species in the steady state on 4 wt.% Ag/Al_2O_3 in a flow of IPA + NO + O_2 at various temperatures. Conditions: NO, 800 ppm; IPA, 1,043 ppm; O_2, 10%. (**c**) In situ DRIFTS spectra of adsorbed species in the steady state on 4 wt.% Ag/Al_2O_3 in a flow of $C_3H_7OH + NO + O_2$ at various temperatures. Conditions: NO, 800 ppm; C_3H_7OH, 1,043 ppm; O_2, 10%. (**d**) In situ DRIFTS spectra of adsorbed species in the steady state on 4 wt.% Ag/Al_2O_3 in a flow of $C_3H_6 + NO + O_2$ at various temperatures. Conditions: NO, 800 ppm; C_3H_6, 1,714 ppm; O_2, 10%. (**e**) In situ DRIFTS spectra of adsorbed species in the steady state on 4 wt.% Ag/Al_2O_3 in a flow of $C_4H_9OH + NO + O_2$ at various temperatures. Conditions: NO, 800 ppm; C_4H_9OH, 783 ppm; O_2, 10%. (**f**) In situ DRIFTS spectra of adsorbed species in the steady state on 4 wt.% Ag/Al_2O_3 in a flow of $CH_3OH + NO + O_2$ at various temperatures. Conditions: NO, 800 ppm; CH_3OH, 3,030 ppm; O_2, 10%. (**g**) In situ DRIFTS spectra of adsorbed species in the steady state on 4 wt.% Ag/Al_2O_3 in a flow of $CH_3OCH_3 + NO + O_2$ at various temperatures. Conditions: NO, 800 ppm; CH_3OCH_3, 3,030 ppm; O_2, 10%

species to form –NCO species [23]. The enolic species was the dominant surface species during partial oxidation of C2–C4 reductants on Ag/Al_2O_3, and it had a high level of reactivity with nitrate species to form –NCO species.

On the basis of the studies described above, we summarize a reaction scheme for NO_x reduction by different reductants over Ag/Al_2O_3, as shown in Scheme 2. For C1 reductants, both formate species and nitrates species adsorbed on Al site are the main intermediates, and they have a low level of reactivity with each other to form –NCO species adsorbed on Ag and Al sites, resulting in a low level of NO_x reduction with C1 reductants over

Table 1 Bands observed on Ag/Al_2O_3 catalysts during DRIFTS experiments and the corresponding surface species and vibrations to which they were assigned (s = symmetric, a = asymmetric, ν = stretching, δ = bending)

Wavenumber (cm^{-1})	Species	Vibration
1585–1589	Normal Al site bidentate nitrate NO_3^-	ν (N=O)
1300–1304	Isolated Al site bidentate nitrate NO_3^-	ν (N=O)
1633–1639	Enolic species RCH=CH–O^-	ν_{as} (RCH=C–O^-)
1412–1416	Enolic species RCH=CH–O^-	ν_s (RCH=C–O^-)
1336–1338	Enolic species RCH=CH–O^-	δ(C–H)
1572–1579	Acetate CH_3OO^-	ν_{as} (COO^-)
1464–1468	Acetate CH_3OO^-	ν_s (COO^-)
1591–1595	Formate $HCOO^-$	ν_{as} (COO^-)
1390–1392	Formate $HCOO^-$	δ(C–H)
1379	Formate $HCOO^-$	ν_s (COO^-)
2229–2239	Isocyanate –NCO	ν_{as} (NCO)

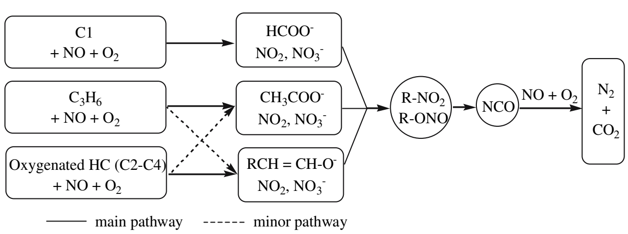

Scheme 2 The proposed mechanisms of the SCR of NO_x by different reductants over Ag/Al_2O_3

Ag/Al_2O_3. For C2, C3 and C4 reductants, the enolic species and the nitrates species adsorbed on Ag and Al sites are the key intermediates, and they have a high level of reactivity with each other to form –NCO species adsorbed on Ag and Al sites, resulting in a high level of NO_x reduction with C2, C3 and C4 reductants over Ag/Al_2O_3. Therefore, C2, C3 and C4 reductants are likely to follow a similar reaction mechanism.

3 Poisoning of SO_2 on the SCR of NO_x with Different Reductants Over Ag/Al_2O_3

3.1 In Situ DRIFTS Study of Adsorbed Sulfate Species on Ag/Al_2O_3

Considering the practical usage of lean NO_x catalysts, sulfur poisoning is one of the key difficulties that must be solved without reducing the NO_x conversion ability of the catalyst [12–16, 33]. SO_2 is considered to be the most important poison for a lean NO_x catalyst because it can react further to form sulfate species, and the accumulation of the sulfate species on the catalyst can lead to a significant loss of catalyst performance. Thus, it is of interest to know how SO_2 influences Ag/Al_2O_3 catalyst. There is still a limited understanding about the formation and configuration of the sulfate species over Ag/Al_2O_3. Here [34], the formation and structure of the sulfate species on Ag/Al_2O_3 were studied in more detail by means of theoretical and experimental vibration spectra.

Figure 4 shows the in situ DRIFTS spectra of Ag/Al_2O_3 at various temperatures in a flow of $SO_2 + O_2$ for a total of 210 min. Two weak bands appeared, at 1,346 cm^{-1} and 1,313 cm^{-1}, after exposing the catalyst to $SO_2 + O_2$ for 30 min at 473 K, and the band at 1,346 cm^{-1} became predominant with increasing exposure time and temperature. According to the literature [32, 34], the bands at 1,346 cm^{-1} and 1,178 cm^{-1} were assigned to surface sulfate species linked to the Al sites, while the band at 1,313 cm^{-1} was probably a similar surface sulfate species linked solely or partly to the Ag site. In addition, there was a distinct shift of the sulfate band from 1,346 cm^{-1} to 1,364 cm^{-1}, which may be caused by the accumulation of sulfate species by the reaction of $SO_2 + O_2$ with Ag/Al_2O_3. A similar experiment was carried out on the surface of pure γ-Al_2O_3 (result not shown). In comparison with the spectra of Ag/Al_2O_3 (Fig. 4), the bands at 1,346 cm^{-1} and 1,178 cm^{-1} were also observed in the spectra of γ-Al_2O_3, indicating that the sulfate species formed mostly on γ-Al_2O_3 [35, 36]. Furthermore, the band at 1,346 cm^{-1} shifting to 1,369 cm^{-1} arising from the accumulation of surface sulfate species was also in good agreement with what has been found in Fig. 4. In addition, the

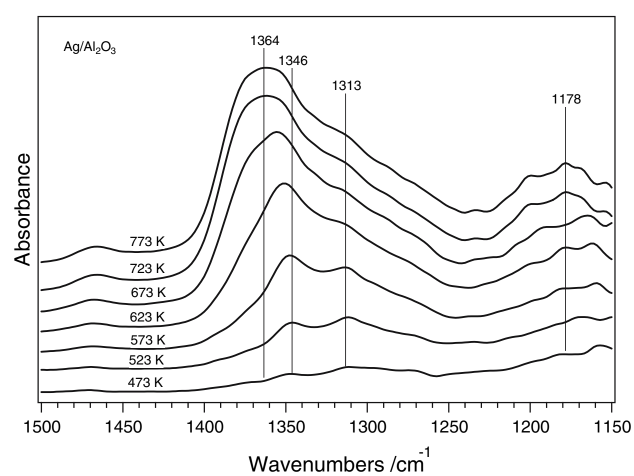

Fig. 4 In situ DRIFTS spectra of adsorbed sulfate species on 4 wt.% Ag/Al_2O_3 in a flow of $SO_2 + O_2$ at various temperatures. Conditions: SO_2, 80 ppm; O_2, 10%

disappearance of 1,313 cm^{-1} peak on pure γ-Al_2O_3 further suggests that this band observed on Ag/Al_2O_3 is related with sulfate species on the Ag site.

To gain insights into the nature of the species formed on the SO_2-poisoned Ag/Al_2O_3, we examined temperature programmed desorption (TPD) curve for Ag/Al_2O_3 after exposure to 80 ppm SO_2 in 10% O_2 at 673 K for 10 h, by monitoring SO_2 ($m/e = 64$) and O_2 ($m/e = 32$) signals. For comparison, TPD pattern of γ-Al_2O_3 poisoned by 80 ppm SO_2 was recorded under the same conditions. As shown in Fig. 5, SO_2 desorbed in two peaks for SO_2-poisoned Ag/Al_2O_3, centered at 889 K and 1,206 K, respectively (top a line). In contrast with SO_2-poisoned Ag/Al_2O_3, the TPD spectrum of SO_2-poisoned γ-Al_2O_3 showed only a peak centered about 1,205 K (bottom b line). These desorption peaks at 889 K and 1,206 K are associated with decomposition of two different kinds of surface sulfate species on Ag/Al_2O_3. According to the literature, $Al_2(SO_4)_3$ was formed through treatment of alumina with SO_2, and it decomposed to yield alumina oxide at 1,073–1,193 K [37]. Compared Fig. 5a and b, the high-temperature peak centered around 1,206 K should be derived from the thermally stable sulfate species formed on the Al site, and its IR bands have been observed at 1,346 cm^{-1} and 1,178 cm^{-1} in Fig. 4. The low-temperature peak centered around 889 K should be attributed to SO_2 decomposed from the sulfate species formed on the Ag site, and its IR band has also been observed at 1,313 cm^{-1} in Fig. 4. Therefore, the TPD results also provide clear evidences for the formation of sulfate species on Ag and Al sites by the reaction of Ag/Al_2O_3 with SO_2.

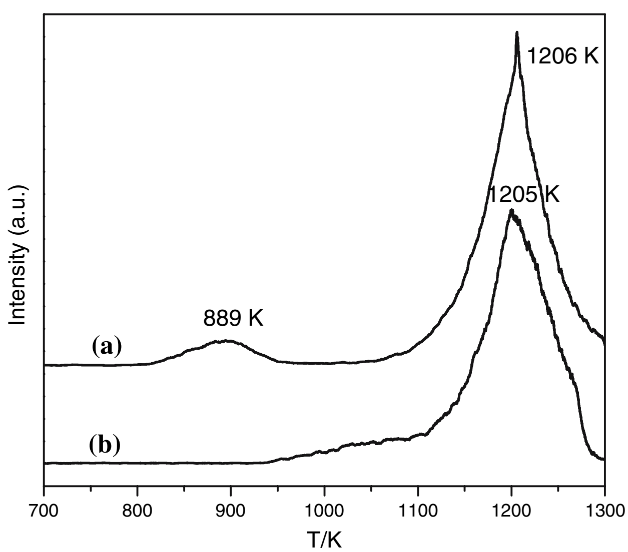

Fig. 5 TPD spectra of SO_2 of 4 wt.% Ag/Al_2O_3 and γ-Al_2O_3 poisoned by 80 ppm SO_2 for 10 h at 673 K: (a) SO_2-poisoned Ag/Al_2O_3 and (b) SO_2-poisoned γ-Al_2O_3

3.2 Conformational Analysis of Adsorbed Sulfate Species on Al_2O_3 by DFT Calculations

As mentioned above, sulfate species were formed mostly on the γ-Al_2O_3 support. Accordingly, we designed bidentate and tridentate models of sulfate species for calculation to obtain a better analysis of the nature of the sulfate species on Al_2O_3, and to explain the phenomenon of the blue shift for the in situ DRIFTS spectra.

The chemical structures of the models calculated for bidentate sulfate species on Al_2O_3 are shown in Fig. 6. Model a was adopted to simulate the lower coverage state, and model b was adopted for the simulation of the higher coverage state. The optimized structures and the simulated

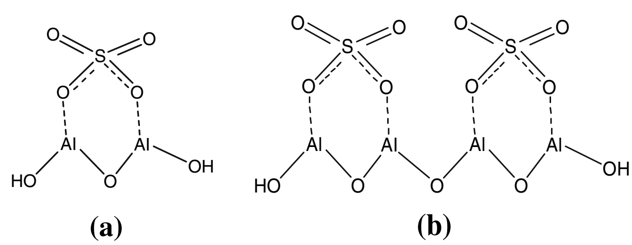

Fig. 6 Models calculated for the bidentate sulfate species formed on Al_2O_3

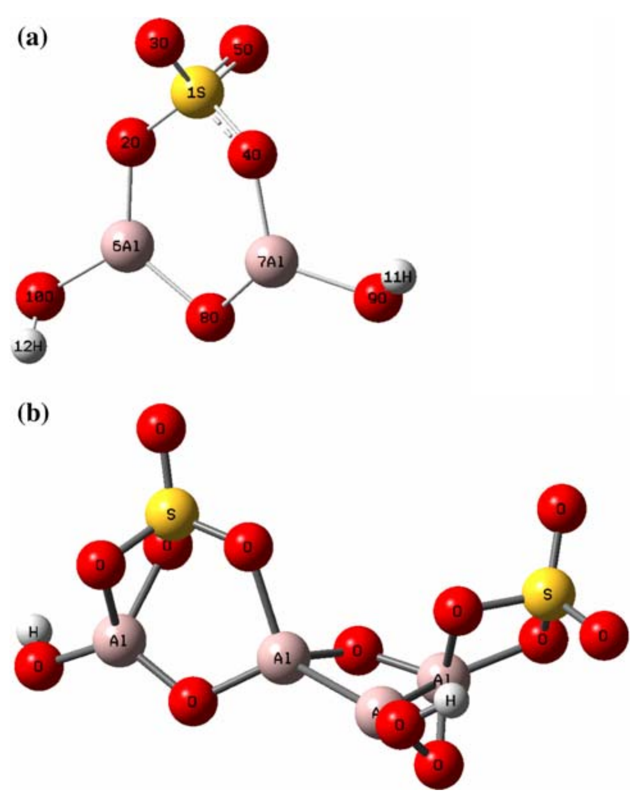

Fig. 7 Optimized configuration of the models calculated for the bidentate sulfate species formed on Al_2O_3

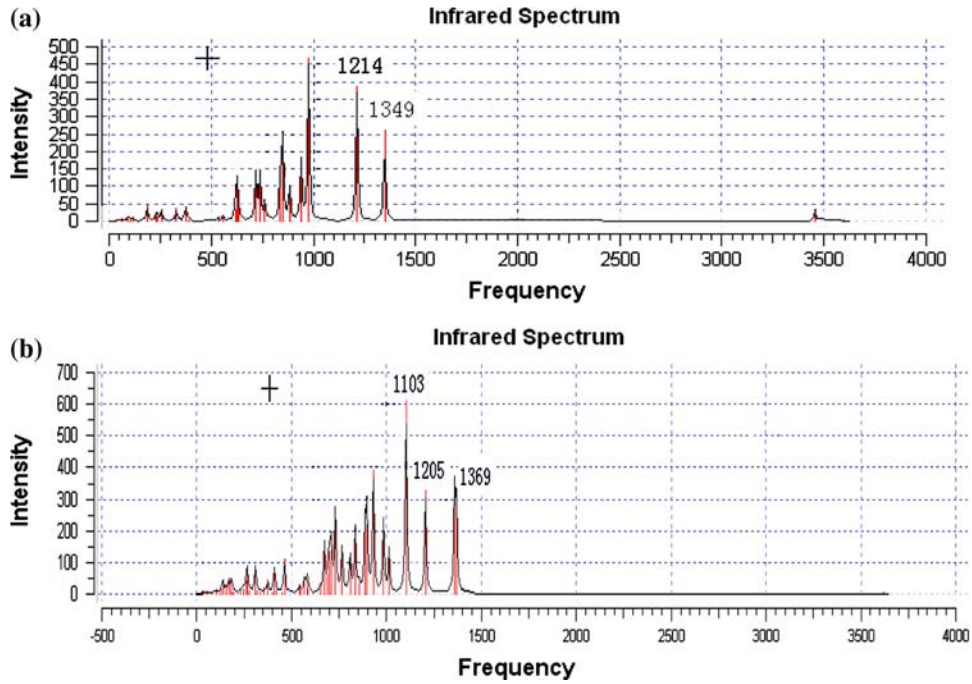

Fig. 8 Calculated vibrational IR spectra for the bidentate sulfate species formed on Al_2O_3

spectra for bidentate sulfate species are presented in Fig. 7 and 8, respectively. As can be seen from Fig. 8a, the ν_{as}(OSO) vibration frequency of model a was calculated as 1,349 cm^{-1} with 260 km/mol intensity, which was close to the experimental value of 1,346 cm^{-1} with strong adsorption, and the ν_s(OSO) vibration frequency of model a was calculated as 1,214 cm^{-1} with 386 km/mol intensity, which was 36 cm^{-1} higher than the experimental value of 1,178 cm^{-1} (Fig. 4). As shown in Fig. 8b, the ν_{as}(OSO) vibration frequency of model b was calculated as 1,369 cm^{-1} with 273 km/mol intensity, which was very close to the experimental value of 1,364 cm^{-1}, and the ν_s(OSO) vibration frequency of model b was calculated as 1,205 cm^{-1} with 327 km/mol intensity, which was 27 cm^{-1} higher than the experimental value of 1,178 cm^{-1} (Fig. 4). When comparing the frequency of the calculated model a with b for bidentate sulfate species, we observe a significant phenomenon; namely, the band shifted from 1,349 cm^{-1} to 1,369 cm^{-1} arising from the accumulation of surface sulfate species, which was in good agreement with the experimental shift of 1,346–1,364 cm^{-1}.

The models of tridentate sulfate species at lower and higher coverage state were calculated in an earlier study [34]. Considering that the calculated results could not be coincident with the real DRIFTS data, the results are not discussed in detail here. Accordingly, from a comparison of theoretical and experimental vibration spectra, it was found that the models of bidentate sulfate species are suitable for investigating the configuration of the sulfate species on Al_2O_3. Moreover, at the lower coverage state, bidentate and tridentate sulfate species might coexist on the surface of the catalyst. The accumulation of sulfate species on the surface could well account for the blue shift of the sulfate species in the IR spectra [34].

3.3 Reaction of Ag/Al_2O_3-Reductant System for the SCR of NO_x in the Presence of SO_2

Earlier, we explained the different influences of SO_2 on the NO_x reduction by C_2H_5OH, C_3H_6 and IPA [16, 32, 38]. Here, the highly efficient systems of Ag/Al_2O_3-C2 reductant (C_2H_5OH), C3 reductants (C_3H_6, IPA, 1-propanol) and C4 reductant (1-butanol) were selected to further study their SO_2 tolerance for practical use.

The effect of SO_2 addition to the feed gas mixture on the SCR activity over Ag/Al_2O_3 was monitored as a function of time on-stream at 673 K and 723 K, which correspond to the temperatures for high NO_x conversions with C2, C3 and C4 reductants. As shown in Fig. 9, in the absence of SO_2, steady-state NO_x conversions of >90% at 673 K were achieved with all of the reaction systems. However, the addition of 80 ppm SO_2 to the feed gas had a different effect on each case. For C3 reductants, NO_x conversion was decreased dramatically compared with C2 and C4 reductants, suggesting that the presence of SO_2 largely deactivates the SCR activity of Ag/Al_2O_3 using C3 reductants. In the case of the C2 reductant, the NO_x conversion was increased slightly at short times, and then passed a maximum to reach a stable level. The final level of NO_x conversion seemed to be influenced slightly by SO_2, indicating that the catalytic system of Ag/Al_2O_3-C2

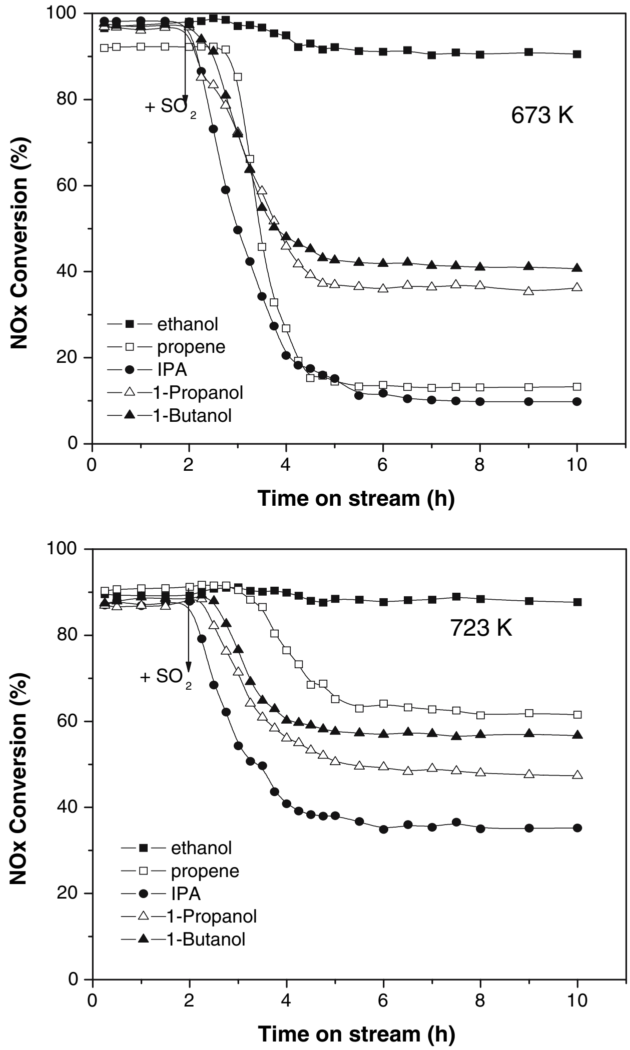

Fig. 9 Effects of SO_2 addition to the feed gas mixture on the SCR activity with different reductants over 4 wt.% Ag/Al_2O_3 were monitored as a function of time on-stream at 673 K and at 723 K. Conditions: NO, 800 ppm; ethanol, 1,565 ppm; or propene, 1,714 ppm; or IPA, 1,043 ppm; or 1-propanol, 1,043 ppm; or 1-butanol, 783 ppm; O_2, 10%; H_2O, 10% in N_2 balance at a total flow rate of 2,000 cm^3/min, GHSV = 50,000 h^{-1}

reductant has the best SO_2 tolerance. By comparison, we can conclude that the Ag/Al_2O_3-C4 reductant catalytic system has the next best SO_2 tolerance. It should be noted that a similar decrease in SCR activity occurred upon addition of 80 ppm SO_2 to the feed gas at 723 K. However, the suppressive effect of SO_2 was smaller than that at 673 K. Thus, we conclude that the reaction temperature is very important in NO_x reduction in the presence of SO_2. In general, the lower the reaction temperature, the greater the negative effect of SO_2.

The results of the activity tests described above showed that the presence of SO_2 in the feed gas can markedly depress the catalytic activity of NO_x reduction for C3 and C4 reductants. In contrast, no pronounced deactivation effect of SO_2 was observed for the C2 reductant under identical experimental conditions. The efficiency order of the reductants for the SCR of NO_x over Ag/Al_2O_3 in the presence of SO_2 is proposed as follows: C2 > C4 > C3. The difference indicates that, in the presence of SO_2, the reaction mechanism of the SCR of NO_x by C2 reductant over Ag/Al_2O_3 is different from that using C3 or C4 reductants.

3.4 SO_2 Poisoning Mechanism in the SCR of NO_x Over Ag/Al_2O_3 by Different Reductants

As mentioned above, the presence of SO_2 can markedly depress the catalytic activity of NO_x reduction for C3 and C4 reductants, while SO_2 hardly affects the catalytic activity of NO_x reduction for the C2 reductant under identical experimental conditions. To gain more information about the sulfur-tolerant catalytic systems, it is crucial to put the emphasis on investigating different mechanisms for each case, as discussed below.

To better investigate the effect of SO_2 on Ag/Al_2O_3 in the flow of different $NO_x + O_2$ + reductant, we performed the in situ DRIFTS experiments as follows: when the reaction reached a steady state (at 60 min), 80 ppm SO_2 was introduced into the feed gas at 673 K. Figure 10a–e show the influence of SO_2 on various catalytic systems at 673 K. The first two spectra in Fig. 10a–e were taken under SO_2-free flow and other spectra were taken in the presence of 80 ppm SO_2 at different time. We can observe that NO_x reduction is influenced strongly by different reductants in the presence of SO_2. When using C_2H_5OH as a reductant (Fig. 10a), no obvious difference was observed among all the spectra by introducing SO_2 into the feed gas. Since there was no sulfate species formed on Ag/Al_2O_3, we can conclude that SO_2 hardly affects the NO_x reduction by C_2H_5OH over Ag/Al_2O_3. This might explain the high efficiency of NO_x reduction with C_2H_5OH over Ag/Al_2O_3 in the presence of SO_2. In the case with IPA as a reductant (Fig. 10b), a new sulfate species peak appeared at 1,342 cm^{-1}, and its intensity increased gradually and shifted to 1,356 cm^{-1}, along with another increasing peak at 1,178 cm^{-1}. At the same time, both the nitrates peak (1,300 cm^{-1}) and the –NCO species peak (2,233 cm^{-1}) decreased in intensity with increased exposure time. The results confirmed that the formation of sulfates species on Ag/Al_2O_3 inhibited the formation of NO_3^-, and suppressed the reaction of enolic species with NO_3^- to form –NCO species, which is responsible for the poor reduction of NO_x with IPA over Ag/Al_2O_3 in the presence of SO_2.

Very similar IR results were obtained for other C3 and C4 reductants, as shown in Fig. 10c–e. In all cases, the formation of surface sulfate species and its negative effect

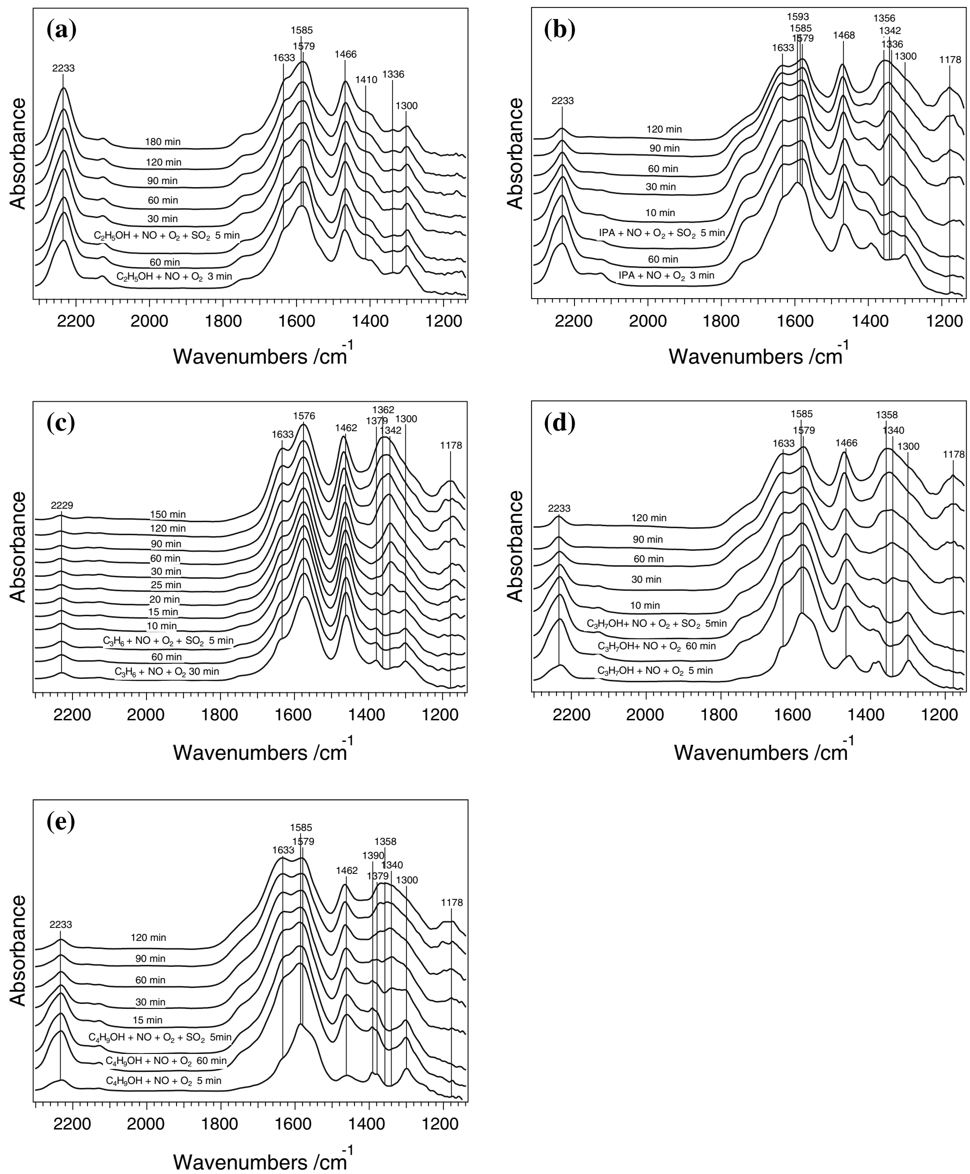

Fig. 10 (**a**) Changes of in situ DRIFTS spectra of adsorbed species on 4 wt.% Ag/Al_2O_3 at 673 K in a flow of $C_2H_5OH + NO + O_2 + SO_2$. Before the measurement, the catalyst was exposed to a flow of $C_2H_5OH + NO + O_2$ for 60 min at 673 K. Conditions: NO, 800 ppm; C_2H_5OH, 1,565 ppm; SO_2, 80 ppm; O_2, 10%. (**b**) Changes of in situ DRIFTS spectra of adsorbed species on 4 wt.% Ag/Al_2O_3 at 673 K in a flow of IPA + NO + O_2 + SO_2. Before the measurement, the catalyst was exposed to a flow of IPA + NO + O_2 for 60 min at 673 K. Conditions: NO, 800 ppm; IPA, 1,043 ppm; SO_2, 80 ppm; O_2, 10%. (**c**) Changes of in situ DRIFTS spectra of adsorbed species on 4 wt.% Ag/Al_2O_3 at 673 K in a flow of $C_3H_6 + NO + O_2 + SO_2$. Before the measurement, the catalyst was exposed to a flow of $C_3H_6 + NO + O_2$ for 60 min at 673 K. Conditions: NO, 800 ppm; C_3H_6, 1,714 ppm; SO_2, 80 ppm; O_2, 10%. (**d**) Changes of in situ DRIFTS spectra of adsorbed species on 4 wt.% Ag/Al_2O_3 at 673 K in a flow of $C_3H_7OH + NO + O_2 + SO_2$. Before the measurement, the catalyst was exposed to a flow of $C_3H_7OH + NO + O_2$ for 60 min at 673 K. Conditions: NO, 800 ppm; C_3H_7OH, 1,043 ppm; SO_2, 80 ppm; O_2, 10%. (**e**) Changes of in situ DRIFTS spectra of adsorbed species on 4 wt.% Ag/Al_2O_3 at 673 K in a flow of $C_4H_9OH + NO + O_2 + SO_2$. Before the measurement, the catalyst was exposed to a flow of $C_4H_9OH + NO + O_2$ for 60 min at 673 K. Conditions: NO, 800 ppm; C_4H_9OH, 783 ppm; SO_2, 80 ppm; O_2, 10%

on the formation of NO_3^- and –NCO species were observed. The results suggested that the SCR activity of NO_x reduction by various C3 or C4 reductants was markedly suppressed by the presence of SO_2. The results were in good agreement with the activity results.

It is worth noting that C2, C3 and C4 alcohols as reductants followed similar mechanisms during the SCR of NO_x. However, in the presence of SO_2, the C2 reductant had the best SO_2 tolerance. This was due to the different enolic species formed from the partial oxidation of different alcohols on Ag/Al_2O_3. We assume that the enolic species formed from the partial oxidation of the C2 reductant contain mainly two carbon atoms [7, 9]. The presence of C2 enolic species could inhibit the formation of sulfate species, therefore the reaction between C2 enolic species and nitrates to form –NCO species on Ag/Al_2O_3 was not influenced by the presence of SO_2. However, the enolic species derived from the partial oxidation of C3 reductants could contain three carbon atoms. The presence of C3 enolic species could not inhibit the formation of sulfate. Therefore, the surface sulfate species inhibited the formation of surface nitrates, which subsequently inhibited the reaction between C3 enolic species and nitrates to form –NCO species on Ag/Al_2O_3. The enolic species originated from the partial oxidation of a C4 reductant mostly contain four carbon atoms, together with a small amount of enolic species containing three or two carbon atoms. Therefore, the catalytic system with a C2 reductant has the best SO_2 tolerance, and that with C4 reductant has the next best SO_2 tolerance, followed by C3 reductants. It is possible that the C2 enolic species has higher reactivity with surface sulfate to reduce it into SO_2 than C3 and C4 enolic species.

The relationship between a catalyst–reductant system and SO_2 tolerance can be described as:

$$SO_2 \text{ tolerance: } Ag/Al_2O_3\text{-C2} \gg Ag/Al_2O_3\text{-C4} > Ag/Al_2O_3\text{-C3}.$$

In general, catalyst composition has been tuned to improve its SO_2 tolerance, with success in many cases, such as V_2O_5/TiO_2. Here, we present a novel idea that it is possible to alter the surface reaction to synthesize a SO_2-resistant surface structure in situ by using different reactants.

4 Effect and the Promotion Mechanism of H_2 on the SCR of NO_x with Different Reductants Over Ag/Al_2O_3

4.1 Effect of H_2 on Catalytic Activity

As discussed above, the Ag/Al_2O_3 catalyst has a very high activity for NO_x reduction by C2, C3 and C4 alcohols. Nevertheless, this catalyst shows a low activity at temperatures below $\sim$600 K for the SCR of NO_x by lower hydrocarbons, and this is a major disadvantage of this technology. H_2 in combination with hydrocarbons has been reported to boost the low-temperature activity of Ag catalysts significantly [20, 21, 39–42]. However, the interpretation of these results is open to debate. On the basis of the previous studies, we have investigated in detail the effect of H_2 on the surface intermediates during the SCR of NO_x by C_3H_6 [43]. Moreover, we were the first to

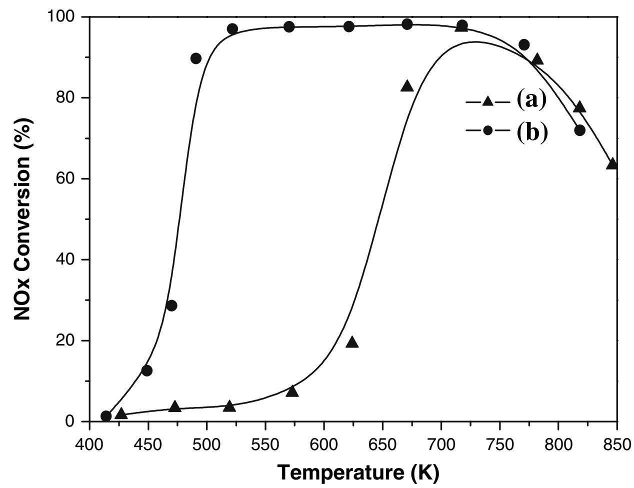

Fig. 11 NO_x conversion (a, b) for the SCR of NO_x by C_3H_6 over 4 wt.% Ag/Al_2O_3 catalyst in the absence of 1% H_2 (a) and in the presence of H_2 (b). Conditions: NO, 800 ppm; C_3H_6, 1,714 ppm; O_2, 10% in N_2 balance at total flow rate 2,000 cm^3/min, GHSV = 50,000 h^{-1}

report the promotional effect of H_2 on the SCR of NO_x by C_2H_5OH [22].

Figures 11 and 12 showed the NO_x conversions for $NO_x/O_2/C_3H_6$ and $NO_x/O_2/C_2H_5OH$ reactions with or without 1% H_2 over Ag/Al_2O_3 catalyst as a function of temperature. As shown in Fig. 11, the NO_x conversion for the SCR of NO_x by C_3H_6 in the absence of H_2 was less than 10% within the temperature range of 423–573 K, and the maximum NO_x conversion of 97% was achieved at 723 K. Clearly, the addition of H_2 enhanced NO_x conversion significantly, especially in the temperature range of 473–623 K. As for the case using C_2H_5OH as a reductant, the reduction of NO_x was also enhanced significantly by the addition of H_2 even if in the presence of H_2O, especially in the temperature range of 423–523 K, as shown in Fig. 12. Compared with the cases without H_2, the NO_x conversion with H_2 was not significantly different from that without H_2 at temperatures higher than 623 K. This is not due to thermodynamic limitation, but due to the selectivity of reductant. At high temperatures, the reaction between the reductant and oxygen resulted in a shortage of C_3H_6 and C_2H_5OH reductants, and H_2 was also consumed totally by oxygen. Therefore, the presence of H_2 could not improve the high-temperature reaction activity.

4.2 GC-MS Analysis of the Effect of H_2 on the Gaseous Products in the SCR of NO_x Over Ag/Al_2O_3

The main gaseous products in the SCR of NO_x by hydrocarbons and oxygenated hydrocarbons over Ag/Al_2O_3

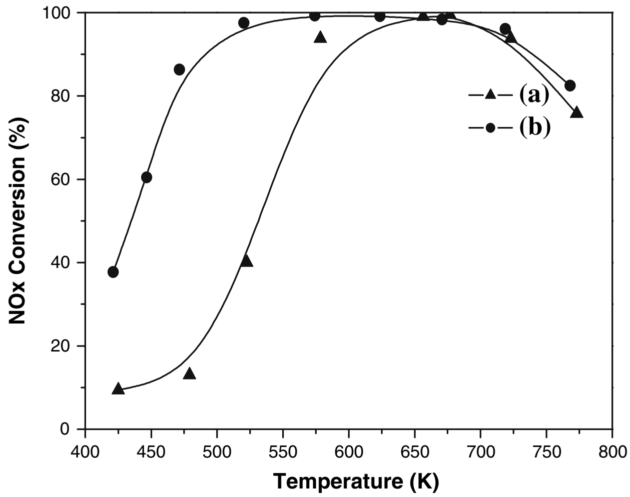

Fig. 12 NO_x conversion (a, b) for the SCR of NO_x by C_2H_5OH over 4 wt.% Ag/Al_2O_3 catalyst in the absence of H_2 (a) and in the presence of 1% H_2 (b). Conditions: NO, 800 ppm; C_2H_5OH, 1,565 ppm; O_2, 10%; H_2O, 10% in N_2 balance at a total flow rate of 2,000 cm^3/min, GHSV = 50,000 h^{-1}

catalyst were N_2, CO_2 and H_2O, accompanied by trace oxygen-containing and nitrogen-containing compounds [3, 10, 17]. Previous studies pointed out that the oxygen-containing and nitrogen-containing compounds could be the intermediates related with the reaction pathway of NO_x reduction [44, 45]. Therefore, it is possible to deduce a reaction pathway by following the origin of trace products. GC-MS measurement was used to monitor these trace products. Figure 13 shows the GC-MS chromatograms of the gas phase products of the SCR of NO_x by C_3H_6 over Ag/Al_2O_3 in the absence or in the presence of H_2 at 473 K in the steady state, respectively. In the absence of H_2, despite small amounts of H_2O and CO_2 detected along with unreacted C_3H_6 and C_3H_8 (impurity), there was no other oxygen-containing and nitrogen-containing compounds observed at 473 K (Fig. 13a). Unlike the case without H_2, the presence of H_2 resulted in the appearance of partial oxidation products of C_3H_6 at same temperature (473 K), such as acetaldehyde and acrolein, accompanied by large amounts of H_2O and CO_2 as final products (Fig. 13b). In addition, traces of CH_3CN and CH_3NO_2 were detected as nitrogen-containing products (Fig. 13b). At temperatures above 573 K, no significant difference in the variety of oxygen-containing and nitrogen-containing compounds was found during the NO_x reduction by C_3H_6 in the presence and in the absence of H_2 (data not shown). These results indicate that the addition of H_2 accelerates the NO_x reduction reaction at low temperatures.

Figure 14a and b show the GC-MS chromatograms of the gas phase products of the SCR of NO_x by C_2H_5OH over Ag/Al_2O_3 in the absence or in the presence of H_2 at 473–623 K in the steady state. The light gaseous molecules,

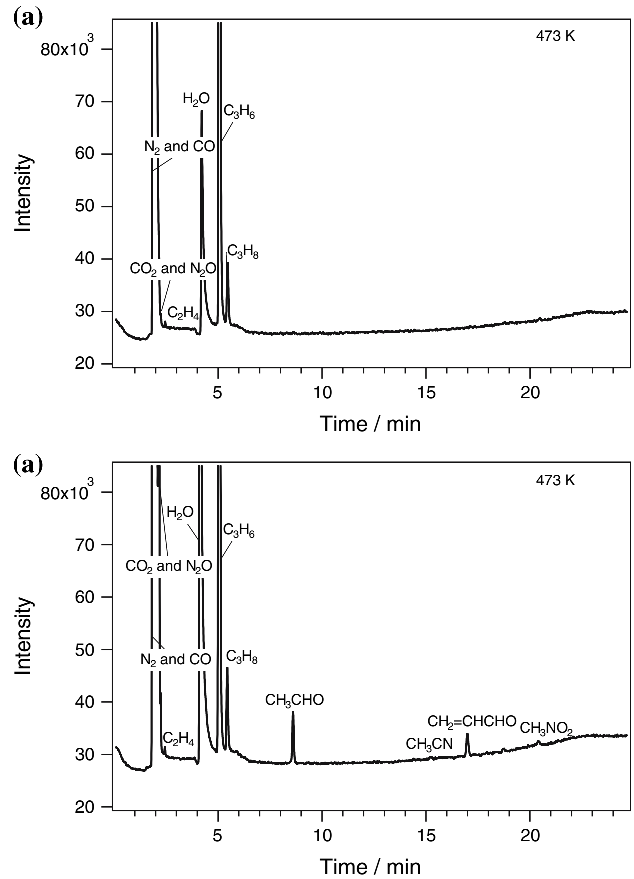

Fig. 13 (**a**) GC-MS chromatogram of gas products of C_3H_6 + NO + O_2 reaction in the absence of H_2 at 473 K over 4 wt.% Ag/Al_2O_3 catalyst. Conditions: NO, 800 ppm; C_3H_6, 1,714 ppm; O_2, 10% in N_2 balance at a total flow rate of 2,000 cm^3/min, GHSV = 50,000 h^{-1}. (**b**) GC-MS chromatogram of gas products of C_3H_6 + NO + O_2 reaction in the presence of 1% H_2 at 473 K over 4 wt.% Ag/Al_2O_3 catalyst. Conditions: NO, 800 ppm; C_3H_6, 1,714 ppm; O_2, 10% in N_2 balance at a total flow rate of 2,000 cm^3/min, GHSV = 50,000 h^{-1}

such as CO_2, N_2O, N_2, and CO, were detected within 5 min retention time and the data were cut from the chromatograms. In the absence of H_2, as shown in Fig. 14a, a small amount of CH_3CHO was detected along with a large amount of unreacted C_2H_5OH, but no other nitrogen-containing compound was observed at 423 K. The intensity of the CH_3CHO peak increased gradually from 423 K to 523 K, and then decreased with further increasing temperature. At 523 K, where ~30% NO_x conversion was achieved (Fig. 12), the production of CH_3CHO was maximized and CH_3NO_2 appeared. At 573 K, CH_3CN appeared, accompanied by a disappearance of CH_3NO_2. However, in the presence of H_2, CH_3CHO was produced in significant amounts reaching a maximum at 423 K, along with the appearance of CH_3NO_2 (Fig. 14b). At 473 K, the disappearance of C_2H_5OH and the traces of CH_3CHO and CH_3NO_2 under these conditions suggested that the reaction proceeded efficiently.

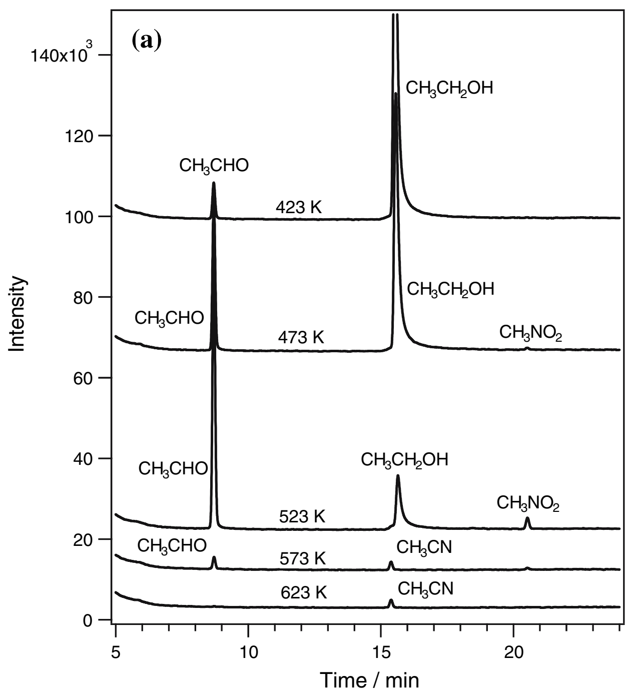

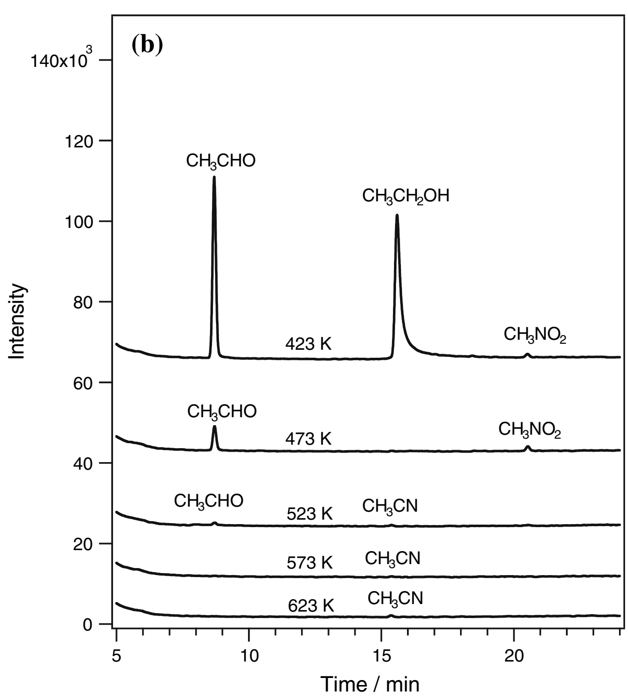

Fig. 14 (**a**) GC-MS chromatogram of gas products of $C_2H_5OH + NO + O_2$ reaction in the absence of H_2 at various temperatures over 4 wt.% Ag/Al_2O_3 catalyst. Conditions: NO, 800 ppm; C_2H_5OH, 1,565 ppm; O_2, 10%; H_2O, 10% in N_2 balance at a total flow rate of 2,000 cm^3/min, GHSV = 50,000 h^{-1}. (**b**) GC-MS chromatogram of gas products of $C_2H_5OH + NO + O_2$ reaction in the presence of 1% H_2 at various temperatures over 4 wt.% Ag/Al_2O_3 catalyst. Conditions: NO, 800 ppm; C_2H_5OH, 1,565 ppm; O_2, 10%; H_2O, 10% in N_2 balance at a total flow rate of 2,000 cm^3/min, GHSV = 50,000 h^{-1}

In comparison with the cases with H_2 (Figs. 13b and 14b) and without H_2 (Fig. 13a and 14a), it is obvious that the presence of H_2 promoted the formation of oxygen-containing molecules (such as CH_3CHO) and nitrogen-containing molecules (such as CH_3NO_2) during the SCR of NO_x by both C_3H_6 and C_2H_5OH. On the basis of the analysis of gas products, it is noticeable that the addition of H_2 significantly promoted the partial oxidation of C_3H_6 or C_2H_5OH to CH_3CHO. As we proposed earlier, enolic surface species ($RCH{=}CH{-}O^-$)-M was formed when CH_3CHO was adsorbed on the surface of Ag/Al_2O_3 [7, 9, 10]. The formation of enolic surface species could be attributed to the CH_3CHO isomerization between the gaseous phase and the catalyst surface. It has been pointed out that the enolic species is related to the efficiency of NO_x reduction by C_2H_5OH or C_3H_6 over Ag/Al_2O_3 [7, 9, 10]. We studied the partial oxidation of C_3H_6 and C_2H_5OH on Ag/Al_2O_3 in the presence of H_2 and its effect on the SCR of NO_x using in situ DRIFTS method, respectively.

4.3 H_2 Promotion Mechanism in the SCR of NO_x by C_2H_5OH or C_3H_6 Over Ag/Al_2O_3

The effect of hydrogen on the formation of surface oxygenated species on Ag/Al_2O_3 was studied by in situ DRIFTS. Figure 15a shows the effect of H_2 on the partial oxidation of C_3H_6 on Ag/Al_2O_3 at 473 K. After exposing Ag/Al_2O_3 to a flow of $C_3H_6 + O_2$ for 180 min, the peak for C=C (1,645 cm^{-1}), a weak peak for enolic species (1,633 cm^{-1}), strong bands for acetate (1,577 cm^{-1} and 1,460 cm^{-1}) and the bands for formate (1591, 1394 cm^{-1}) were observed [7, 9, 10, 23, 30–32]. The bands due to acetate were predominant at 473 K in the absence of H_2. When H_2 was added to the flow of $C_3H_6 + O_2$ at the same temperature, the bands due to adsorbed acetate (1,577 cm^{-1} and 1,460 cm^{-1}) were similarly observed on Ag/Al_2O_3. However, it should be noted that the peak at 1,633 cm^{-1} for enolic species intensified gradually as a function of time, accompanied by the appearance of other peaks at 1,413 cm^{-1} and 1,336 cm^{-1} of the enolic species. After flowing H_2 for 60 min, the peak at 1,633 cm^{-1} achieved maximum intensity. Accordingly, the enolic species and acetate became the predominant surface species in the presence of H_2.

For using C_2H_5OH as a reductant, similar results were observed, as shown in Fig. 15b. After exposing Ag/Al_2O_3 to a flow of $C_2H_5OH + O_2$ for 30 min at 423 K, the peaks of enolic species (1,635 cm^{-1}), acetate (1,579 cm^{-1} and 1,460 cm^{-1}) and δ(C–H) of adsorbed acetate (1,392 cm^{-1})

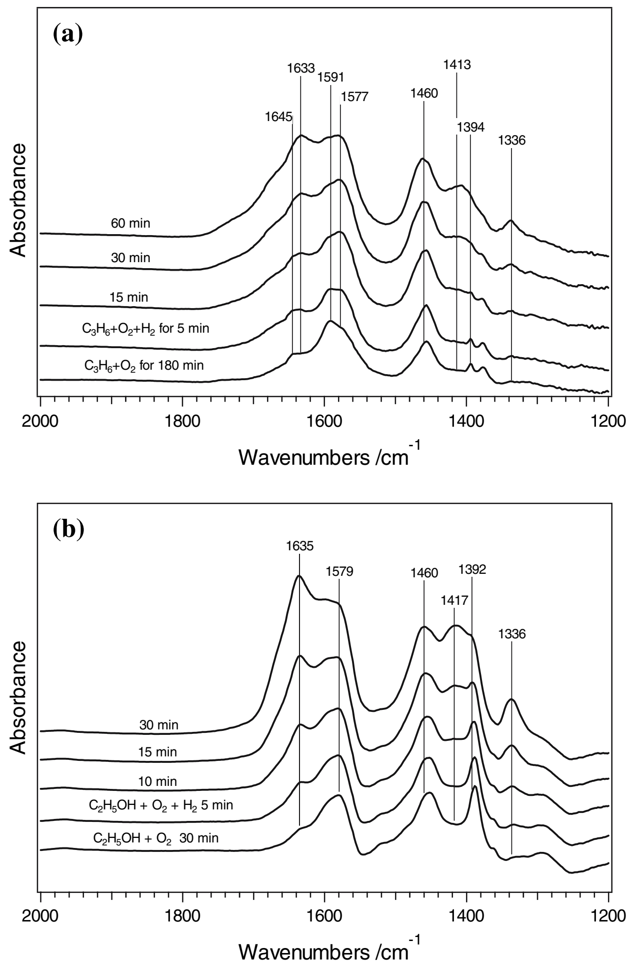

Fig. 15 (**a**) Dynamic changes of in situ DRIFTS spectra of 4 wt.% Ag/Al_2O_3 as a function of time in a flow of $C_3H_6 + O_2 + H_2$ at 473 K. Before the measurement, the catalyst was exposed to a flow of $C_3H_6 + O_2$ for 180 min at 473 K. Conditions: C_3H_6, 1,714 ppm; O_2, 10%; H_2, 1%. (**b**) Dynamic changes of in situ DRIFTS spectra of 4 wt.% Ag/Al_2O_3 as a function of time in a flow of $C_2H_5OH + O_2 + H_2$ at 423 K. Before the measurement, the catalyst was exposed to a flow of $C_2H_5OH + O_2$ for 30 min at 423 K. Conditions: C_2H_5OH, 1,565 ppm; O_2, 10%; H_2, 1%

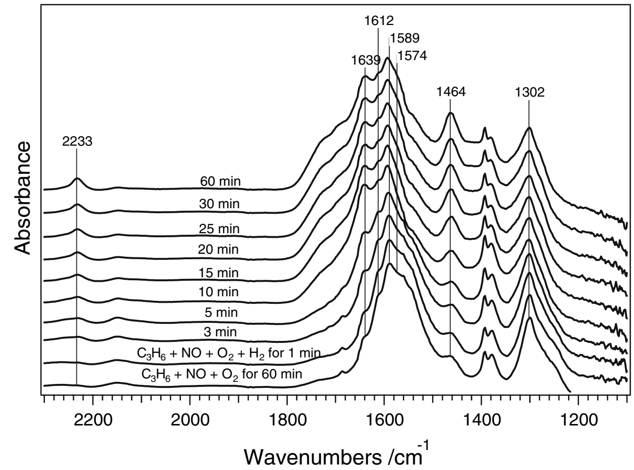

Fig. 16 Dynamic changes of in situ DRIFTS spectra of 4 wt.% Ag/Al_2O_3 as a function of time in a flow of $C_3H_6 + NO + O_2 + H_2$ at 523 K. Before the measurement, the catalyst was exposed to a flow of $C_3H_6 + NO + O_2$ for 60 min at 523 K. Conditions: NO, 800 ppm; C_3H_6, 1,714 ppm; O_2, 10%; H_2, 1%

were observed on Ag/Al_2O_3 [7, 9, 10, 23, 30–32, 46]. When H_2 was added to the flow of $C_2H_5OH + O_2$ at 423 K, it should be noted that the band intensity of enolic species (1,635 cm^{-1}, 1,417 cm^{-1} and 1,336 cm^{-1}) increased gradually as a function of time. After flowing H_2 for 30 min, the peak at 1,635 cm^{-1} achieved maximum intensity, indicating that enolic species became the predominant surface species. On the basis of these observations, it is suggested that the presence of H_2 promotes the partial oxidation of C_3H_6 and C_2H_5OH, especially the formation of enolic species at low temperature. In our previous study [43], we proposed that the molecular oxygen might be activated by the addition of H_2 over Ag/Al_2O_3 catalyst, forming a peroxo-like species. This species is highly active oxidant, and favorable to the partial oxidation of reductants.

To elucidate the effect of H_2 on the SCR of NO_x by C_3H_6, we investigated dynamic changes of the reaction intermediates on the Ag/Al_2O_3 by DRIFTS. Figure 16 shows the in situ DRIFTS spectra of Ag/Al_2O_3 in a flow of $C_3H_6 + NO + O_2$ and then $C_3H_6 + NO + O_2 + H_2$. After exposing the catalyst to a flow of $C_3H_6 + NO + O_2$ for 60 min at 523 K, the enolic species (1,639 cm^{-1}), nitrates (1,589 cm^{-1} and 1,302 cm^{-1}) and acetate (1,574 cm^{-1} and 1,464 cm^{-1}) were observed. By examining the intensity of each peak under a flow of $C_3H_6 + NO + O_2$, the nitrates (1,589 cm^{-1} and 1,302 cm^{-1}) appeared to dominate on Ag/Al_2O_3 at this temperature. After adding H_2 to the mixture of $C_3H_6 + NO + O_2$, the bands of adsorbed nitrates (1,589 cm^{-1} and 1,302 cm^{-1}) and acetate (1,574 cm^{-1} and 1,464 cm^{-1}) were still visible on Ag/Al_2O_3 at the same temperature, whereas the surface concentrations of the enolic species (1,639 cm^{-1}) and –NCO species (2,233 cm^{-1}) increased significantly with time. These results suggest strongly that the presence of H_2 enhances the formation of enolic species and –NCO species during the SCR of NO_x. Considering the high reactivity of the enolic species with nitrates [7, 9, 10], it is reasonable that the formation of –NCO surface species is promoted in the presence of H_2.

Similar in situ DRIFTS studies were performed in the SCR of NO_x by C_2H_5OH. Figure 17 shows the in situ DRIFTS spectra of Ag/Al_2O_3 in a flow of $C_2H_5OH + NO + O_2$ and then $C_2H_5OH + NO + O_2 + H_2$. Compared with the case without H_2, the significant change was that the surface concentration of the enolic species

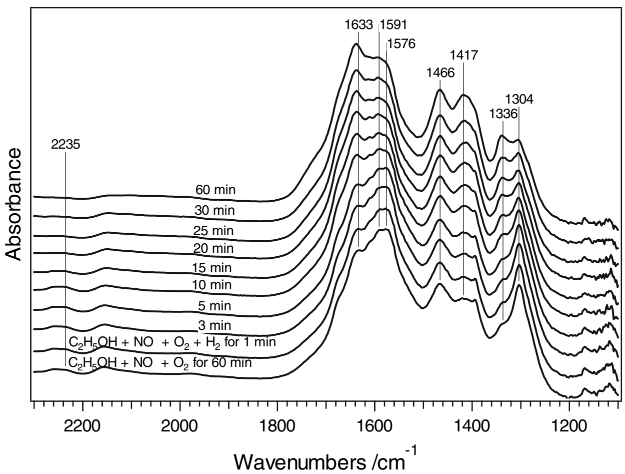

Fig. 17 Dynamic changes of in situ DRIFTS spectra of 4 wt.% Ag/Al_2O_3 as a function of time in a flow of C_2H_5OH + NO + O_2 + H_2 at 473 K. Before the measurement, the catalyst was exposed to a flow of C_2H_5OH + NO + O_2 for 60 min at 473 K. Conditions: NO, 800 ppm; C_2H_5OH, 1,565 ppm; O_2, 10%; H_2, 1%

(1,633 cm^{-1}, 1,417 cm^{-1} and 1,336 cm^{-1}) increased significantly with time, and the peaks associated with this species became the most intense among all absorbed species peaks in 20 min. This result suggests strongly that the presence of H_2 facilitates the formation of enolic species during the NO_x reduction by C_2H_5OH, even at very low temperature. Another obvious difference was that the bands for surface bidentate nitrates (1,591 cm^{-1} and 1,304 cm^{-1}) decreased with time, indicating low steady-state nitrates coverage in the presence of H_2. Compared to the case with C_3H_6 as a reductant in the presence of H_2 (Fig. 16), the peak at 2,235 cm^{-1} assigned to –NCO decreased with time in the presence of H_2. We postulated that –NCO could participate in the formation of other active species in the presence of H_2, which was responsible for the enhancement of NO_x conversion.

To obtain further information on the effect of H_2 on the whole reaction, the reactions of –NCO with NO + O_2, with and without the addition of H_2, were further investigated by in situ DRIFTS. After treating Ag/Al_2O_3 in C_2H_5OH + NO + O_2 for 60 min at 523 K, as shown in Fig. 18a and b, a peak at 2,233 cm^{-1} for –NCO and a peak at 2,154 cm^{-1} for –CN were observed [17, 31]. As seen in Fig. 18a, when C_2H_5OH flow was interrupted, continual monitoring of the adsorbed species on Ag/Al_2O_3 in the flow of NO + O_2 revealed that –NCO and –CN did not react with NO + O_2 in 30 min at 523 K. However, as shown in Fig. 18b, the intensity of the adsorbed –NCO bands decreased and disappeared in 20 min, indicating a strong reactivity of the adsorbed –NCO species in the flow of NO + O_2 + H_2 at this temperature. It is noticeable that a new peak at 1,612 cm^{-1} in Fig. 18b appeared gradually,

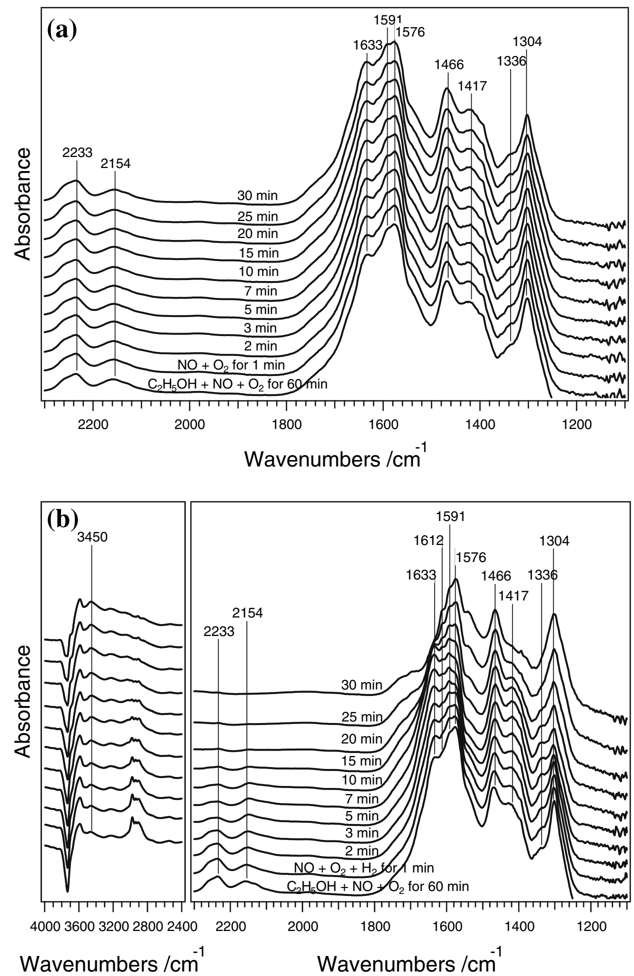

Fig. 18 (**a**) Dynamic changes of in situ DRIFTS spectra of 4 wt.% Ag/Al_2O_3 in a flow of NO + O_2 as a function of time at 523 K. Before the measurement, the catalyst was exposed to a flow of C_2H_5OH + NO + O_2 for 60 min at 523 K. Conditions: NO, 800 ppm; C_2H_5OH, 1,565 ppm; O_2, 10%. (**b**) Dynamic changes of in situ DRIFTS spectra of 4 wt.% Ag/Al_2O_3 in a flow of NO + O_2 + H_2 as a function of time at 523 K. Before the measurement, the catalyst was exposed to a flow of C_2H_5OH + NO + O_2 for 60 min at 523 K. Conditions: NO, 800 ppm; C_2H_5OH, 1,565 ppm; O_2, 10%; H_2, 1%

accompanied by the disappearance of –NCO, and this new peak may be due to a deformation mode of adsorbed NH_x on Ag/Al_2O_3 [47, 48]. At the same time, a weak peak was observed at 3,450 cm^{-1}, which may be assigned to the stretching vibration mode of NH species [49]. On the basis of the results described above, the consumption of –NCO species may be related to the rapid hydrolysis of –NCO species in the flow of NO + O_2 + H_2, resulting in the formation of NH_x species.

On the basis of the results of the experiments and the mechanism proposed previously, we summarize a simplified reaction scheme for the reduction of NO_x by C_3H_6 and C_2H_5OH in the presence of H_2. As shown in Scheme 3, the

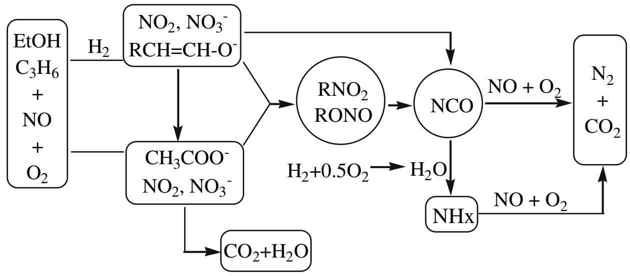

Scheme 3 The possible effect of H_2 on the SCR of NO_x by C_3H_6 and C_2H_5OH over Ag/Al_2O_3

presence of H_2 first promotes the partial oxidation of C_3H_6 and C_2H_5OH to enolic species. Subsequently, in the case of C_3H_6 as a reductant, the presence of H_2 accelerates the reaction between enolic species and nitrates to form key intermediates –NCO, and then enhances the reactions of enolic species and –NCO towards NO + O_2 to form N_2 as a final product. These lead to the corresponding enhancement of Ag/Al_2O_3 in the SCR of NO_x by C_3H_6 in the presence of H_2. As for C_2H_5OH as a reductant, besides the promotion effects mentioned above, the presence of H_2 further promotes the hydrolysis of –NCO to form NH_x species, which was known to be highly active towards NO_x reduction when using NH_3 as a reductant over Ag/Al_2O_3 in the presence of H_2 [50]. Therefore, the formation of NH_x species may be another reason that the addition of H_2 improves the reaction activity of NO_x reduction by C_2H_5OH.

5 Application of Ag/Al_2O_3–C_2H_5OH–SCR System to a Heavy-duty Diesel Engine

5.1 Honeycomb Catalyst Engine Test

On the basis of the results obtained under laboratory conditions, we found that the Ag/Al_2O_3 catalyst exhibits a high activity for the SCR of NO_x with C_2H_5OH in the presence of H_2O and SO_2, and the best performance of Ag/Al_2O_3 is achieved with 4% Ag loading [7]. Therefore, a bench test was carried out using the Ag/Al_2O_3 washcoated honeycomb catalyst and C_2H_5OH as a reducing agent on a diesel engine under practical operating condition [19].

In order to investigate the influence of the exhaust gas temperature and GHSV of a honeycomb catalyst on NO_x conversion, the impact of the exhaust components and THC (total hydrocarbons)/NO_x ratio should be eliminated. Therefore, the engine was operated in the same mode at 3,450 rpm at full load in the following experiments. The THC/NO_x ratio in effluent gas was fixed at 3.4 by C_2H_5OH injection. The temperature at the inlet of the catalyst was adjusted by the heat exchanger, and GHSV was changed by the bypass valve.

Figure 19 shows the catalytic activity of the Ag/Al_2O_3 honeycomb catalyst (SCR catalyst) with different GHSVs (30,000 h^{-1}, 50,000 h^{-1}, 80,000 h^{-1}) at a fixed THC/NO_x ratio of 3.4. As shown in Fig. 19a, the honeycomb catalyst showed a very high activity for the removal of NO_x at the GHSV of 30,000 h^{-1}. The maximal conversion of NO_x was up to 93%, and the average conversion of NO_x was ~77% in the wide temperature range of 543–743 K. Those results are similar to our results in the laboratory-scale test, which indicates that Ag/Al_2O_3 has a realistic potential in reducing NO_x under real diesel engine exhaust conditions. Increasing the GHSV from 30,000 h^{-1} to 50,000 h^{-1} and 80,000 h^{-1}, the catalytic activity for the removal of NO_x was decreased gradually. The curve of NO_x conversion was shifted towards higher temperatures, and the average conversion of NO_x was only ~52% in the wide temperature range of 593–763 K at a GHSV of 80,000 h^{-1}. Figure 19b shows that THC conversions have no obvious change with the increase of GHSV. In addition, as shown in Fig. 19c, CO conversion was observed as negative value, indicating that CO was produced during the SCR of NO_x by C_2H_5OH. It can be seen that the negative CO conversion decreased with the increase of GHSV from 30,000 h^{-1} to 50,000 h^{-1} and 80,000 h^{-1}. Since CO production is in direct proportion to the NO_x conversion, we propose that CO is not produced mainly from partial oxidation of HC, but from the C_2H_5OH-SCR of NO_x process.

5.2 EURO III ESC Test of Honeycomb Catalysts

In order to make the original Sofim 8140-43 C EURO II diesel engine meet EURO III standards, the catalytic system for the removal of NO_x was tested and optimized at the 13-mode test cycle for heavy-duty diesel engines.

Table 2 shows the EURO III ESC test results with different catalysts. It should be noted that the C_2H_5OH was not injected at idle speed. It can be seen that the NO_x emission is much lower than that of the original engine over the SCR catalyst, which meets the EURO III regulation. However, the amount of the by-products such as CO, unburned THC increased and exceeded the EURO III limits. The increase of CO and unburned THC was due to the addition of ethanol as the reducing agent during the bench test on the HC-SCR-fitted engine. As a result, certain measures should be taken to reduce HC and CO simultaneously, such as using an oxidation catalyst with a low light-off temperature, or optimizing the strategy of the C_2H_5OH addition.

According to our previous research results [10], a Cu/Al_2O_3 honeycomb oxidation catalyst was added directly

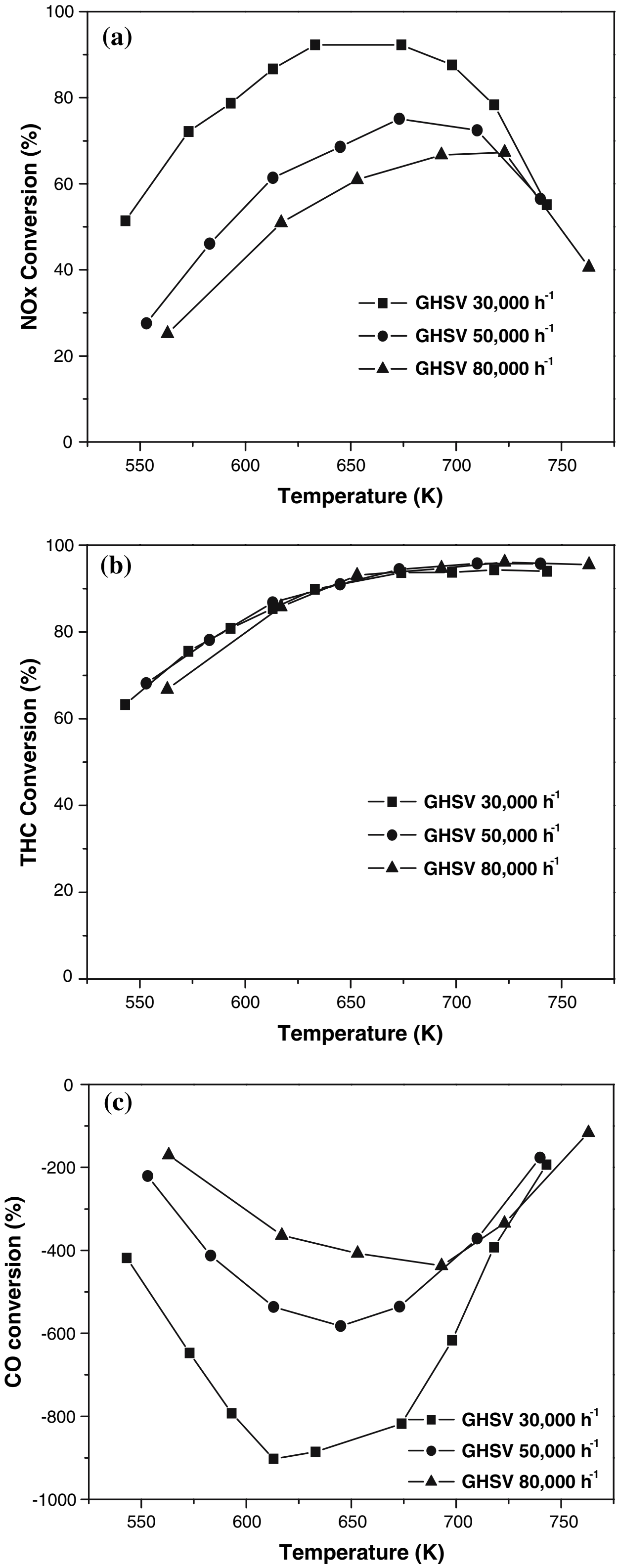

Fig. 19 Effect of GHSV (30,000 h^{-1} (■), 50,000 h^{-1} (●), 80,000 h^{-1} (▲)) on the catalytic activity. (**a**) NO_x conversion, (**b**) THC conversion, (**c**) CO conversion. Operating conditions: engine speed 3450 rpm, torque 195 Nm (full load), THC/NO_x ratio 3.4

Table 2 EURO III ESC test results

Emissions	CO (g/kW h)	THC (g/kW h)	NO_x (g/kW h)
EURO III limits	2.1	0.66	5.0
Original engine	1.307	0.355	6.924
SCR	3.482	1.431	2.668
SCR + Oxi	0.098	0.709	3.654

after the SCR catalyst to reduce THC and CO. It can be seen from Table 2 that the SCR + Oxi composite catalyst reduced NO_x emission, and CO emission was much lower than the EU limits. The HC emission was also reduced from more than twice the limit to just a little higher. Therefore, the SCR + Oxi composite catalyst is more effective than a single SCR catalyst for meeting EURO III regulations. However, because the HC emission still does not meet the EURO III standard, the addition of C_2H_5OH should be optimized.

As shown in Fig. 19a, the SCR catalyst showed a high level of activity for NO_x reduction only in the middle range of temperatures, such as 573–723 K. At lower temperatures (<573 K), the NO_x conversion was lower, and the addition of C_2H_5OH caused a great increase of THC emission without obviously improving the NO_x conversion. In this case, without adding C_2H_5OH, the THC emission would be reduced greatly, although the NO_x emission would be increased slightly. At higher temperatures (>723 K), NO_x conversion was also very low. In this case, ambient temperature air could be introduced into the exhaust pipe to reduce the temperature of the exhaust gas to within the temperature range of high NO_x conversion, and then the NO_x conversion would be increased.

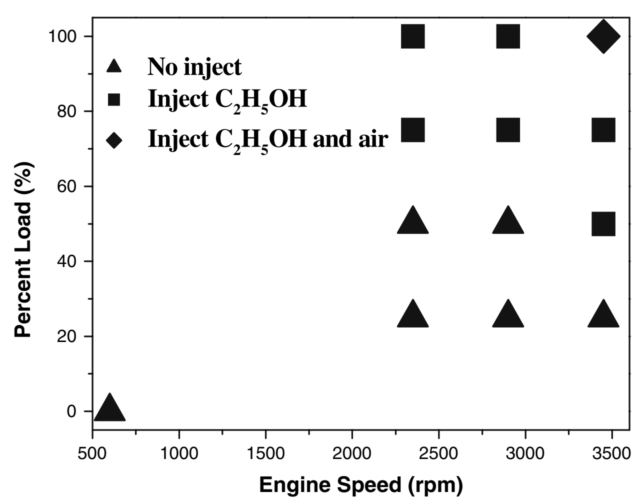

Fig. 20 The optimization of C_2H_5OH addition

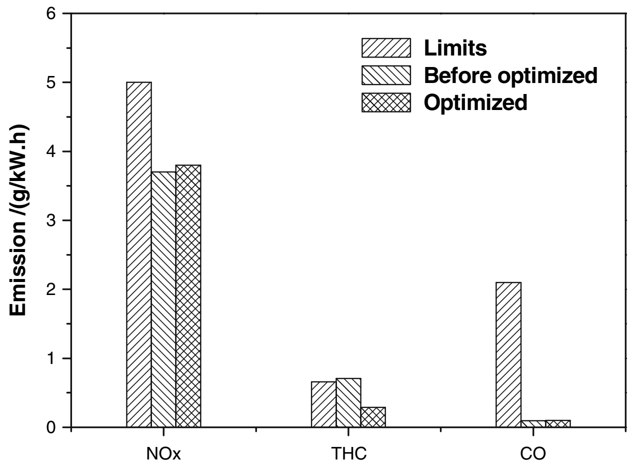

Fig. 21 Test results after optimization of C_2H_5OH addition

According to the 13 operating conditions of EURO III ESC [19], the exhaust temperatures were relatively low at modes 1, 3, 5, 7, 9 and 11, so C_2H_5OH was not added due to the low NO_x emission and conversion. On the other hand, adequate C_2H_5OH was added for NO_x reduction at the high conversion temperature range of modes 2, 4, 6, 8, 12 and 13. In addition, the exhaust temperature was too high at mode 10, so ambient temperature air was introduced along with the addition of C_2H_5OH. The strategy of C_2H_5OH addition is shown in Fig. 20.

The EURO III ESC test results after optimization are shown in Fig. 21. It was shown that NO_x and CO emissions are nearly the same as that before optimization, but HC emission is greatly reduced, making the Sofim 8140-43 C diesel engine emissions meet EURO III standards.

6 Conclusion

In this review, the SCR of NO_x with different reductant over Ag/Al_2O_3 and its application on the diesel engine exhaust cleaning were summarized. The effective order of the oxygenated reductants for the SCR of NO_x over Ag/Al_2O_3 is proposed as follows: C4 reductants $\approx$ C2 reductants > C3 reductants >> C1 reductants. Using C1 reductants, both formate species and nitrate species are the main intermediates, and they have a low level of reactivity with each other to form –NCO species, resulting in low NO_x reduction with C1 reductants over Ag/Al_2O_3. Using C2 or C3 or C4 reductants, the enolic species and nitrates species are the key intermediates, and they have a high level of reactivity with each other to form –NCO species, resulting in high NO_x reduction with C2, C3 and C4 reductants over Ag/Al_2O_3.

The formation of sulfate species on the catalyst resulted in a decrease of the active sites. The comparison between theoretical and experimental vibration spectra enabled us to draw the following conclusions: bidentate sulfate species rather than tridentate sulfate species are the predominant surface species on Ag/Al_2O_3. The accumulation of surface sulfate species could well explain the phenomenon of the blue shift in the IR spectra.

Activity tests showed that the presence of SO_2 in the feed gas can markedly depress the catalytic activity of NO_x reduction with C3 and C4 reductants. Evidence from the in situ DRIFTS spectra shows that the presence of sulfate species on Ag/Al_2O_3 not only inhibited the formation of NO_3^-, but also inhibited the reaction of enolic species with NO_3^- to form –NCO species, which was responsible for the deactivation of Ag/Al_2O_3 during the SCR of NO_x with C3 and C4 reductants in the presence of SO_2. In contrast, no pronounced deactivation effect of SO_2 was observed when C2 oxygenated reductant was used under the identical experimental conditions. The C2 enolic species formed from the partial oxidation of C2 reductants can inhibit the formation of sulfate species on Ag/Al_2O_3 in the presence of SO_2. The relationship between catalyst–reductant system and SO_2 tolerance can be described as below:

$$SO_2 \text{ tolerance: } Ag/Al_2O_3\text{-C2} \gg Ag/Al_2O_3\text{-C4} > Ag/Al_2O_3\text{-C3}.$$

In this way, we provide a new idea that it is possible to alter surface reaction to synthesize a SO_2-resistant surface structure in situ by using different reactants.

The activity of the SCR of NO_x by hydrocarbon over Ag/Al_2O_3 was enhanced significantly by the addition of H_2, especially in the low temperature range of 473–623 K. The addition of H_2 promoted the formation of enolic species during the partial oxidation of hydrocarbon over Ag/Al_2O_3 catalyst at low temperature. According to our previous studies, this certainly led to the corresponding enhancement of Ag/Al_2O_3 in the SCR of NO_x in the presence of H_2. The addition of H_2 also promoted significantly the activity of NO_x reduction by oxygenated hydrocarbon over Ag/Al_2O_3 with a promotional mechanism similar to that mentioned above. As for C_2H_5OH as a reductant, the presence of H_2 promoted the formation of enolic species during the partial oxidation of C_2H_5OH, and the formation of another active NH_x species by the hydrolysis of –NCO.

Since the Ag/Al_2O_3-C2 reductant system has extremely high efficiency for the SCR of NO_x and high SO_2 tolerance, it was used for catalytic cleaning of NO_x in diesel exhaust. Compared with the Ag/Al_2O_3 granule catalyst, the Ag/Al_2O_3 washcoated honeycomb catalyst (SCR catalyst) had a similar activity for NO_x reduction by C_2H_5OH in the diesel engine bench test. Using the Cu/Al_2O_3 washcoated NO_x catalyst as the oxidation catalyst and matching with the optimization of C_2H_5OH addition, the SCR + Oxi composite catalyst can effectively remove the NO_x, THC and CO from diesel exhaust and make the emission meet EURO III standards under the 13-mode test cycle.

Acknowledgements This work was financially supported by the National Science Fund for Distinguished Young Scholars of China (20425722), Key Program of NNSFC (20437010) and Ministry of Science and Technology of China (2006AA060304).

References

1. PaÃrvulescua VI, Grange P, Delmon B (1998) Catal Today 46:233
2. Miyadera T (1993) Appl Catal B 2:199
3. Miyadera T (1997) Appl Catal B 13:157
4. Nakatsuji T, Yasukawa R, Tabata K, Ueda K, Niwa M (1998) Appl Catal B 17:333
5. Eränen K, Lindfors LE, Niemi A, Elfving P, Cider L (2000) SAE Technical Paper Series 2000-01-2813
6. Lindfors LE, Eränen K, Klingstedt F, Murzin DY (2004) Top Catal 28:185
7. He H, Yu YB (2005) Catal Today 100:37
8. Shimizu K, Satsuma A (2006) Phys Chem Chem Phys 8:2677
9. Yu YB, He H, Feng QC (2003) J Phys Chem B 107:13090
10. Yu YB, He H, Feng QC, Gao HW, Yang X (2004) Appl Catal B 49:159
11. Sumiya S, He H, Abe A, Takezawa N, Yoshida K (1998) J Chem Soc Faraday Trans 94:2217
12. Meunier FC, Ross JRH (2000) Appl Catal B 24:23
13. Satokawa S, Yamaseki K, Uchida H (2001) Appl Catal B 34:299
14. Park PW, Boyer CL (2005) Appl Catal B 59:27
15. Houel V, James D, Millington P, Pollington S, Poulston S, Rajaram R, Torbati R (2005) J Catal 230:150
16. Wu Q, Gao HW, He H (2006) Chin J Catal 27:403
17. Sumiya S, Saito M, He H, Feng QC, Takezawa N, Yoshida K (1998) Catal Lett 50:87
18. Abe A, Aoyama N, Sumiya S, Kakuta N, Yoshida K (1998) Catal Lett 51:5
19. Zhang CB, He H, Shuai SJ, Wang JX (2007) Environ Pollut 147:415
20. Satokawa S (2000) Chem Lett 294
21. Burch R, Breen JP, Hill CJ, Krutzsch B, Konrad B, Jobson E, Cider L, Eränen K, Klingstedt F, Lindfors LE (2004) Top Catal 30/31:19
22. Zhang XL, He H, Ma ZC (2007) Catal Commun 8:187
23. Wu Q, He H, Yu YB (2005) Appl Catal B 61:107
24. Bhattacharyya S, Das RK (1999) Int J Energy Res 23:351
25. Fritz A, Pitchon V (1997) Appl Catal B 13:1
26. Webster DE (2001) Top Catal 16/17:33
27. Ukisu Y, Sato S, Abe A, Yoshida K (1993) Appl Catal B 2:147
28. Bion N, Saussey J, Haneda M, Daturi M (2003) J Catal 217:47
29. Kameoka S, Ukisu Y, Miyadera T (2000) Phys Chem Chem Phys 2:367
30. Shimizu K, Shibata J, Yoshida H, Satsuma A, Hattori T (2001) Appl Catal B 30:151
31. Meunier FC, Zuzaniuk V, Breen JP, Olsson M, Ross JRH (2000) Catal Today 59:287
32. Wu Q, He H, Feng QC, Yu YB (2006) Catal Commun 7:657
33. Xie GY, Liu ZY, Zhu ZP, Liu Q, Ge J, Huang ZG (2004) J Catal 224:36
34. Wu Q, Gao HW, He H (2006) J Phys Chem B 110:8420
35. Waqlf M, Saur O, Lavalley JC (1991) J Phys Chem 95:4051
36. Goodman AL, Li P, Usher CR, Grassian VH (2001) J Phys Chem 105:6109
37. Tabata M, Tsuchida H, Miyamoto K, Yoshinari T, Yamazaki H, Hamada H, Kintaichi Y, Sasaki M, Ito T (1995) Appl Catal B 6:169
38. Wang J, He H, Xie SX, Yu YB (2005) Catal Commun 6:195
39. Satokawa S, Shibata J, Shimizu K, Satsuma A, Hattori T (2003) Appl Catal B 42:179
40. Richter M, Bentrup U, Eckelt R, Schneider M, Pohl MM, Fricke R (2004) Appl Catal B 51:261
41. Sazama P, Čapek L, Drobná H, Sobalík Z, Dědeček J, Arve K, Wichterlová B (2005) J Catal 232:302
42. Klingstedt F, Arve K, Eränen K, Murzin DYu (2006) Acc Chem Res 39:273
43. Zhang XL, Yu YB, He H (2007) Appl Catal B 76:241
44. Gorce O, Baudin F, Thomas C, Costa PD, Djéga-Mariadassou G (2004) Appl Catal B 54:69
45. Cant NW, Cowan AD, Liu IOY, Satsuma A (1999) Catal Today 54:473
46. Martínez-Arias A, Fernández-García M, Iglesias-Juez A, Anderson JA, Conesa JC, Soria J (2000) Appl Catal B 28:29
47. Ramis G, Yi L, Busca G, Turco M, Kotur E, Willey RJ (1995) J Catal 157:523
48. Macleod N, Lambert RM (2003) Appl Catal B 46:483
49. Sato K, Yoshinari T, Kintaichi Y, Haneda M, Hamada H (2003) Appl Catal B 44:67
50. Richter M, Fricke R, Eckelt R (2004) Catal Lett 94:115